

# Polyoxoanion-supported catalysis: evidence for a $P_2W_{15}Nb_3O_{62}^{9-}$ -supported iridium cyclohexene oxidation catalyst starting from $[n\text{-Bu}_4N]_5Na_3[(1,5\text{-COD})Ir \cdot P_2W_{15}Nb_3O_{62}]$

Heiko Weiner<sup>1</sup>, Alessandro Trovarelli<sup>2</sup>, R.G. Finke\*

Department of Chemistry, Colorado State University, Fort Collins, CO 80523-1872, USA

Received 10 December 2001; accepted 29 May 2002

## Abstract

The polyoxoanion-supported iridium complex  $[n\text{-Bu}_4N]_5Na_3[(1,5\text{-COD})Ir \cdot P_2W_{15}Nb_3O_{62}]$ , **1**, was previously shown to be an active homogeneous catalyst for cyclohexene oxidation catalysis via a classic, Haber–Weiss ROO ( $R = 2\text{-cyclohexen-1-yl}$ ) free-radical-chain autoxidation mechanism. The question posed in the present work is: “Is the true catalyst polyoxoanion-supported?”, an important question given that polyoxoanion-supported catalysts are one of only eight new conceptual subclasses of polyoxoanions in catalysis developed over the last ca. 20 years. The present work probes the above question via a range of methods, specifically: catalytic activity and kinetic studies; isolation of the catalyst following the reaction and characterization of the catalyst by transmission electron microscopy (TEM), elemental analysis, IR, nuclear magnetic resonance, ultracentrifugation and fast atom bombardment mass spectrometry molecular weight methods, plus ion-exchange resin tests to provide evidence for inner-sphere attachment of the oxidized  $Ir^{n+}$  moiety to the  $P_2W_{15}Nb_3O_{62}^{9-}$  polyoxoanion. The results suggest “ $[(n\text{-Bu}_4N)_6Na_3(HO)_3Ir^{3+} \cdot P_2W_{15}Nb_3O_{62}]_x$  ( $x = 1, 2$ )” as a *working model* for the average molecular formula of the catalyst. Most importantly, the results are definitive in answering the question posed: the true catalyst is polyoxoanion-supported. This finding is of significance since the autoxidation of cyclohexene beginning with  $[n\text{-Bu}_4N]_5Na_3[(1,5\text{-COD})Ir \cdot P_2W_{15}Nb_3O_{62}]$ , **1**, is, historically, the first bona fide example of a polyoxometalate-supported catalyst and, hence, the first demonstration of a new subclass of polyoxoanion-based catalysts. However, a remaining challenge is the development of more important oxidations or other chemistries from polyoxoanion-supported catalysts.

© 2002 Published by Elsevier Science B.V.

**Keywords:** Polyoxoanions; Polyoxoanion-supported catalysis; Homogeneous catalysis; Cyclohexene oxidation catalysis; Molecular oxygen; Catalyst isolation and characterization; Mechanistic studies

## 1. Introduction

Polyoxoanions [1–3] can be described as discrete fragments of close-packed, solid oxide structures

of the general formula  $M_xO_y$  (M: metal, O: oxygen), a resemblance first noted by Baker [4]. Such solid oxides are well established, key components of metal oxide-supported, heterogeneous-insoluble<sup>3</sup>

\* Corresponding author. Fax: +1-970-491-1801.

E-mail address: rfinke@lamar.colostate.edu (R.G. Finke).

<sup>1</sup> Present address: Dow Chemical Corporation, 3200 Kanawha Turnpike, South Charleston, WV 25303, USA.

<sup>2</sup> Present address: Dipartimento di Scienze e Tecnologie Chimiche, Università di Udine, via Cotonificio 108, Udine, Italy.

<sup>3</sup> Schwartz has proposed definitions that limit a homogeneous catalyst to one with a single, chemically unique (i.e., homogeneous) active site, and a heterogeneous catalyst to one with multiple, chemically different (i.e., heterogeneous) catalytically active sites [4]. Schwartz further suggests the addition of the suffix-soluble or -insoluble for single-phase or multiphase systems, respectively.

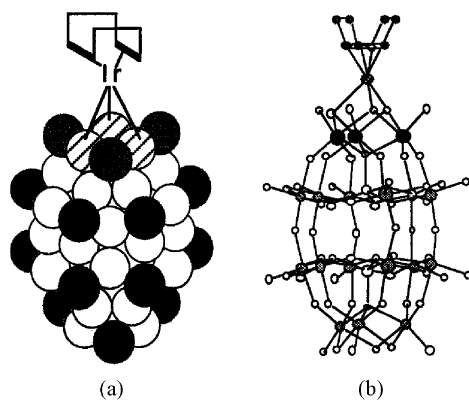
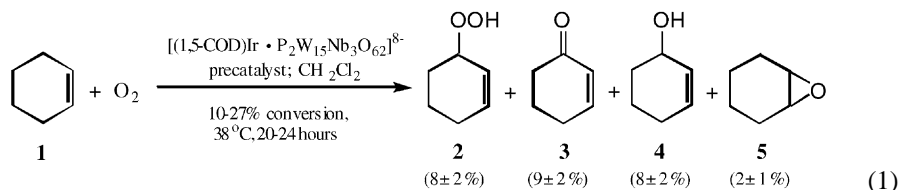


Fig. 1. (a) Space filling representation of the [(1,5-COD)Ir]<sup>+</sup> fragment supported on the “Nb<sub>3</sub>O<sub>6</sub>” face of [n-Bu<sub>4</sub>N]<sub>9</sub>P<sub>2</sub>W<sub>15</sub>Nb<sub>3</sub>O<sub>62</sub>, where the black circles represent terminal oxygens, the white circles bridging oxygen, the black circles adjacent to the hatched circles are terminal Nb–O oxygens, and the hatched circles are the three Nb–O–Nb oxygens. (b) Ball and stick representation of [n-Bu<sub>4</sub>N]<sub>5</sub>Na<sub>3</sub>[(1,5-COD)Ir-P<sub>2</sub>W<sub>15</sub>Nb<sub>3</sub>O<sub>62</sub>] with the P<sub>2</sub>W<sub>15</sub>Nb<sub>3</sub>O<sub>62</sub><sup>9-</sup> polyoxometalate serving as stereochemically rigid tripodal ligand.

[5] catalysts. For some time now we [6,7] have been interested in using the organic-solvent soluble [1b,8] tetraalkylammonium salts of M = Nb(V), V(V), or Ti(IV) Dawson-type trisubstituted polyoxoanions, P<sub>2</sub>W<sub>15</sub>M<sub>3</sub>O<sub>62</sub><sup>n-</sup> which, therefore, have surface oxygen basicity (i.e., anionic surface charge-density)<sup>4</sup>



and, hence, are able to support organometallic complexes atop their surface oxygen. (See also Klemperer’s [9] pioneering work in polyoxometalate-supported complexes using, for example, the smaller hexametalate, Nb<sub>2</sub>W<sub>4</sub>O<sub>19</sub><sup>4-</sup> system.)

Within this context it is, therefore, *homogeneous-soluble* and *homogeneous-insoluble* catalysts that are of greatest current interest in catalysis due to the expectation that they will exhibit the most selective and active catalytic chemistries.

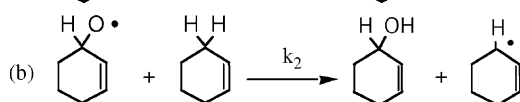
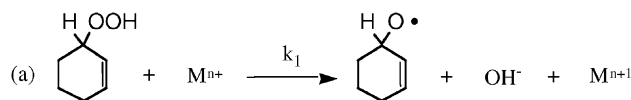
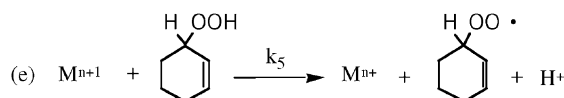
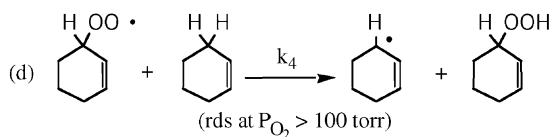
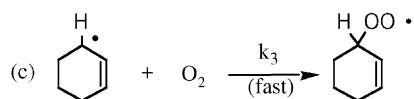
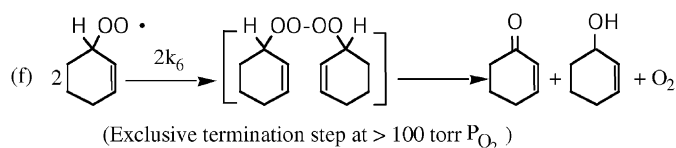
<sup>4</sup> It is worth mentioning the difference between the custom-made, *basic* P<sub>2</sub>W<sub>15</sub>Nb<sub>3</sub>O<sub>62</sub><sup>9-</sup> vs. the commercially available, well known, and *acidic* polyoxoanions PW<sub>12</sub>O<sub>40</sub><sup>3-</sup> or P<sub>2</sub>W<sub>18</sub>O<sub>62</sub><sup>6-</sup> which parallel ClO<sub>4</sub><sup>-</sup> in their conjugate acid strength.

Previously, we reported the synthesis of the polyoxometalate iridium complex [n-Bu<sub>4</sub>N]<sub>5</sub>Na<sub>3</sub>[(1,5-COD)Ir-P<sub>2</sub>W<sub>15</sub>Nb<sub>3</sub>O<sub>62</sub>], **1** (Fig. 1) [10]. This prototype, Dawson-supported polyoxoanion complex has been characterized by <sup>1</sup>H, <sup>13</sup>C, <sup>31</sup>P, and <sup>183</sup>W nuclear magnetic resonance (NMR) spectroscopy as well as IR spectroscopy, sedimentation-equilibrium molecular weight measurements, and complete elemental analysis. A single crystal X-ray structure on its parent, P<sub>2</sub>W<sub>15</sub>Nb<sub>3</sub>O<sub>62</sub><sup>9-</sup> polyoxoanion exists as well [7b]. A direct demonstration using <sup>17</sup>O NMR of the Ir–O–Nb support attachment of the (1,5-COD)Ir(I)<sup>+</sup> in **1** has also been published [11].

Our longer term interest in polyoxoanion-supported organometallic complexes is in learning what catalytic chemistry<sup>5</sup> can result from using them as novel pre-catalysts. In 1991 we described the first reports using polyoxoanion-supported complexes as effective pre-catalysts for both reductive [12] and oxidative [13] catalysts, including patents in each area [12b,13b]. In the oxidative catalysis area, we reported that [(1,5-COD)Ir-P<sub>2</sub>W<sub>15</sub>Nb<sub>3</sub>O<sub>62</sub>]<sup>8-</sup> served as an effective pre-catalyst for cyclohexene oxidation (Eq. (1)) [13], research which *appeared* to have discovered the first polyoxoanion-*supported* catalyst, thereby providing a new subclass of polyoxoanion-based catalysts, one of only eight new subclasses discovered during the last ca. 20 years (see Fig. 1 elsewhere [14])<sup>6</sup>

<sup>5</sup> These polyoxoanion-supported analogs are not intended to replace or even to closely “model” polymetallic metal cluster particles supported on solid oxides. Instead, they are new materials that are novel compositions of matter. It follows that they will exhibit their own unique chemistry and reactivity in at least some reactions (and that they will also exhibit unique *disadvantages* under some conditions; see footnote 5 elsewhere [6j]). Hence, our main goal is to create a prototype example which illustrates of both the advantages and disadvantages of this new subclass of polyoxoanion-based catalysts.

<sup>6</sup> Reviews of heteropolyoxoanions in homogeneous and heterogeneous catalysis is given in Ref. [15]. A series of 34 recent papers in a volume devoted to polyoxoanions in catalysis is given in Ref. [15b]. See also the chapters beginning in p. 113, 171, 199 and 219 is given in Ref. [15g].

**INITIATION****PROPAGATION****TERMINATION**

Scheme 1. The classic Haber–Weiss [17] radical-chain sequence mechanism for cyclohexene autoxidation reported in Eq. (1) and based on the product, kinetic and mechanistic work reported elsewhere [16].

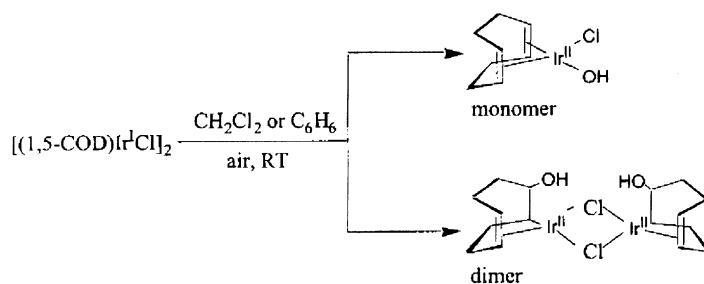
More recently we have studied the reaction kinetics and mechanism of the cyclohexene oxidation in Eq. (1) in some detail. The results of those studies [16] provide unequivocal evidence that the reaction is autoxidation via a classic, Haber–Weiss mechanism [16,17] (Scheme 1).

Hence, we know that the [(1,5-COD)Ir-P<sub>2</sub>W<sub>15</sub>Nb<sub>3</sub>O<sub>62</sub>]<sup>8-</sup> precatalyst is evolving, under the oxidizing conditions of the reaction (Eq. (1)), into a catalyst whose main function is to serve as an electron-transfer chain initiator, M<sup>n+</sup>/M<sup>n+1</sup>, Scheme 1, step (a), and resultant alkylhydroperoxide oxidizer (M<sup>n+1</sup>/M<sup>n+</sup>), step (e). We also know from our initial work [12] that the presence of the [P<sub>2</sub>W<sub>15</sub>Nb<sub>3</sub>O<sub>62</sub>]<sup>9-</sup> polyoxoanion is important, accelerating the rate of autoxidation (Eq. (1)) by ca. 100-fold in the absence of any added cyclohexene hydroperoxide initiator. Hence,

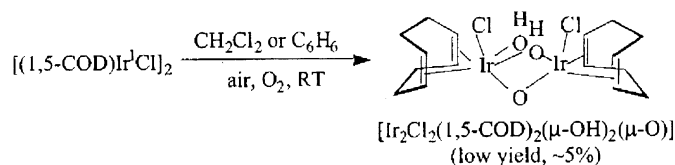
it is likely that the true catalyst is indeed polyoxoanion-supported, and the polyoxoanion P<sub>2</sub>W<sub>15</sub>Nb<sub>3</sub>O<sub>62</sub><sup>9-</sup> is probably accelerating the redox reaction by facilitating oxidation of the Ir<sup>I</sup> to Ir<sup>n+</sup> and shifting the resultant Ir<sup>n+/n+1</sup> redox potential to more positive values.

However, it is important to obtain more evidence for, or against, the true catalyst being the first example of a polyoxoanion-supported catalyst<sup>7</sup> [18]—especially since polyoxoanion-supported catalysts are

<sup>7</sup> Other reports of catalysis have appeared [18] with mixtures containing certain types of polyoxoanions and organo transition metal complexes. However, in each case the active catalyst, although quite interesting, is clearly not a tightly supported transition metal–polyoxoanion complex either by design, or due to the use of polyoxoanions with negligible or insufficient surface oxygen charge-density.



Scheme 2. Proposed, but unverified, monomeric and dimeric, Ir<sup>II</sup> structures for “[IrC<sub>8</sub>H<sub>13</sub>ClO]<sub>x</sub>”, obtained by air-oxidation of [(1,5-COD)IrCl]<sub>2</sub> [20a].



Scheme 3. Air-oxidation of [(1,5-COD)IrCl]<sub>2</sub> in dichloromethane or benzene to yield the X-ray crystallographically characterized, bimetallic complex, [(1,5-COD)<sub>2</sub>Ir<sub>2</sub>O(OH)<sub>2</sub>Cl<sub>2</sub>] [20b].

still rare and, hence, little studied [14]. Obtaining just such evidence, is the primary goal of the present paper.

First, however, it is useful to summarize the relevant literature on the evolution of Ir<sup>I</sup> olefin complexes under dioxygen,<sup>8</sup> especially since some of that literature is for a P<sub>3</sub>O<sub>9</sub><sup>3-</sup>-supported (1,5-COD)Ir<sup>+</sup> complex, namely [(1,5-COD)Ir·P<sub>3</sub>O<sub>9</sub>]<sup>2-</sup>, and since we have found that this complex behaves catalytically quite similarly to our own [(1,5-COD)Ir·P<sub>2</sub>W<sub>15</sub>Nb<sub>3</sub>O<sub>62</sub>]<sup>8-</sup> complex.

## 2. Relevant literature background

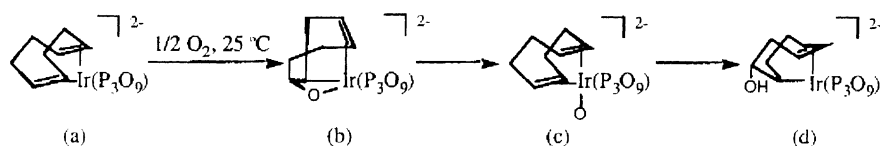
There is only a small amount of literature, specifically papers by Bonnaire and Fourgeroux [20a], Cotton et al. [20b], and Klemperer and others [21], in which reactions of 1,5-COD iridium complexes with molecular oxygen or air are reported. In 1975, Bonnaire and Fourgeroux [20a] reported the air-oxidation of [(1,5-COD)IrCl]<sub>2</sub> in dichloromethane and benzene leading to the empirical [IrC<sub>8</sub>H<sub>13</sub>(Cl)(O)]·1/2 S (S:

<sup>8</sup> Several other iridium complexes are known to be active in oxygenation reactions; for lead references see Ref. [19].

dichloromethane, benzene). Possible monomeric and dimeric structures (Scheme 2) are discussed in this study based on IR and Raman spectroscopy, and elemental analysis. Unfortunately, no molecular weight data were reported, however. Note that both of the proposed structures in Scheme 2 involve a less common, formally Ir<sup>II</sup> (d<sup>7</sup>) oxidation state; however, the expected paramagnetism was also not confirmed experimentally [20a].

In 1986, Cotton et al. [20b] reported a second study of the air-oxidation of [(1,5-COD)IrCl]<sub>2</sub> in dichloromethane as well as in benzene; a low yield of approximately 5% of a dimeric, diamagnetic Ir(III) complex, [(1,5-COD)<sub>2</sub>Ir<sub>2</sub>O(OH)<sub>2</sub>Cl<sub>2</sub>] (Scheme 3) was confirmed by X-ray crystallography of the solvate complex, [(1,5-COD)<sub>2</sub>Ir<sub>2</sub>O(OH)<sub>2</sub>Cl<sub>2</sub>]·1/2 CH<sub>2</sub>Cl<sub>2</sub>.

In perhaps the study most relevant to the present work, in 1990, Klemperer and co-workers [21a] reported the stoichiometric oxidation of the 1,5-COD iridium complex, [(1,5-COD)Ir·P<sub>3</sub>O<sub>9</sub>]<sup>2-</sup>, by molecular oxygen in acetonitrile or 1,2-dichloroethane. Using <sup>31</sup>P NMR spectroscopy, three oxygen-containing species were identified. One of these, an oxametallacyclobutane complex, [(C<sub>8</sub>H<sub>12</sub>O)Ir·P<sub>3</sub>O<sub>9</sub>]<sup>2-</sup> was verified by X-ray crystallography; this intermediate



Scheme 4. The 1,5-cyclooctadiene complex  $[(C_8H_{12}O)Ir\cdot P_3O_9]^{2-}$  (a), was found to react stoichiometrically with 0.5 equiv.  $O_2$ , yielding first a oxametallacyclo complex (identified by NMR spectroscopy) (b), the isomeric oxo-complex (c), is then converted into the hydroxylated allyl complex  $[(C_8H_{11}OH)Ir\cdot P_3O_9]^{2-}$  (d) [21a]. The oxo-complex  $[(C_8H_{12})(O)Ir\cdot P_3O_9]^{2-}$  (a), could also be converted to the corresponding aquo complex  $[(C_8H_{12})(OH_2)Ir\cdot P_3O_9]$  (not shown) by the addition of trichloroacetic acid [21c].

is converted into an isomer, the allyl complex  $[(C_8H_{11}OH)Ir\cdot P_3O_9]^{2-}$  (Scheme 4).

In an additional study, Klemperer and others [21b] reported the comparison of oxidation of  $\eta^4$ -cyclooctadiene iridium(I) complexes of  $P_3O_9^{3-}$  and  $Cp'\{Cp' = 1, 3-C_5H_3(SiMe_3)_2\}$ , only now in the radical-chain-supporting solvent 1,1,2,2-tetrachloroethane (see Ref. [10] in [21b]). Investigations of the reaction of  $[(1,5-COD)IrCp']$  with oxygen implicate a free-radical-chain mechanism of 1,5-cyclooctadiene ligand oxidation resulting in two isomeric, 1,5-cyclooctadiene-derived, but still Ir coordinated, ketone complexes. The different behavior of the cyclooctadiene iridium(I) complex of  $P_3O_9^{3-}$  in its stoichiometric reaction with oxygen (leading to two  $[(C_8H_{12}O)Ir\cdot P_3O_9]^{2-}$  isomers, cf., Scheme 4) is attributed by Klemperer and others [21b] to the flexidentate  $P_3O_9^{3-}$  ligand, which can easily adopt a  $\kappa^2$ -O-bonding mode in  $[(C_8H_{12})Ir(P_3O_9)]^{2-}$  producing a 16 electron species capable of oxidatively adding  $O_2$ , a highly plausible, but kinetically untested, hypothesis. Due to structural similarities between  $[(1,5-COD)Ir\cdot P_3O_9]^{2-}$ ,  $[(1,5-COD)IrCp']$  and the  $[(1,5-COD)Ir\cdot P_2W_{15}Nb_3O_{62}]^{8-}$  examined herein, these interesting, albeit stoichiometric, reactions with  $O_2$  reported by Klemperer et al. provide the closest available precedent for the initial reactions with oxygen of the present  $[(1,5-COD)Ir\cdot P_2W_{15}Nb_3O_{62}]^{8-}$  system.

Other, hydroxo- and oxo-bridged species involving iridium and rhodium organometallics are known [22a–i]. Relatively stable tri- $\mu$ -hydroxo-diiridium and rhodium complexes have been described for  $[M(C_5Me_5)_2(OH)_3][B(C_6H_5)_4]$  ( $M = Ir, Rh$ ). Both structures show two metal atoms, each  $\eta^5$ -bonded to the  $C_5Me_5$  ( $=Cp^*$ ) ligand and bridged by three hydroxo ligands [22a–e]. Their catalytic activity in oxygena-

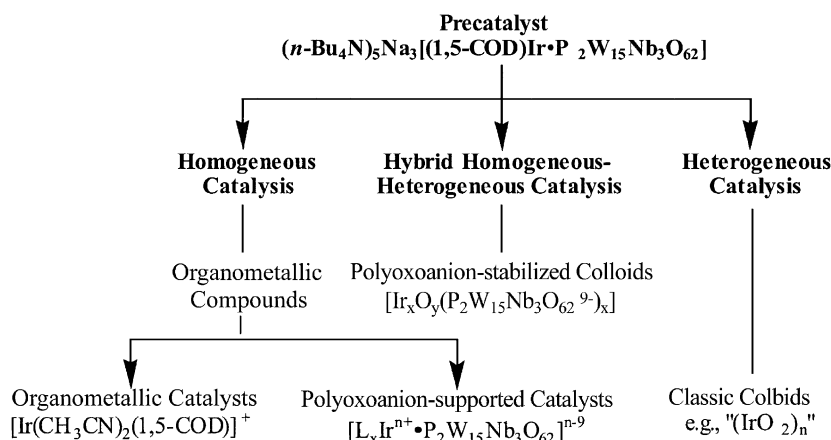
tion reactions (e.g., tetrahydrofuran to  $\gamma$ -butyrolactone and oxidation of triphenylphosphine) have been reported previously [22i]. Bergman has described a  $Cp^*Ir(\mu_2-O)_2IrCp^*$  precursor which, upon  $H_2O$  addition, yields the monocation,  $[Cp^*Ir(\mu_2-OH)_3IrCp^*]^+$  [22f]. Trimeric iridium- $\mu^3$ -oxo-bridged clusters have also been reported [22f]. Peroxo complexes of Ir(III) are fairly common, and have been shown to oxidize a variety of reactive substrates such as CO or primary alcohols, ROH [23] (see also [26]).

### 3. Results and discussion

#### 3.1. The central issue: Is the true catalyst polyoxoanion-supported?

The use of polyoxoanion-supported transition metals such as  $[(1,5-COD)Ir\cdot P_2W_{15}Nb_3O_{62}]^{8-}$  as precatalysts leads naturally to the central issue surrounding the resultant catalysts: is the true, active catalyst still polyoxoanion-supported?; has the organometallic moiety leached off, for example, making the polyoxoanion nothing more than an overly complicated precatalyst? This plus several other conceivable reaction pathways which might account for the observed catalysis are summarized in Scheme 5. Refuting, or supporting, these possibilities forms a basis for the experiments done to answer the key question: “Is the true catalyst polyoxoanion-supported?”

To address the question of the nature of the true catalyst, and to distinguish between the above possibilities, we returned to a methodology that we first developed and used elsewhere to distinguish between homogeneous and heterogeneous catalysts (in that



Scheme 5. Conceivable reaction pathways for the observed autoxidation catalysis starting with the polyoxoanion-supported catalyst precursor,  $[n\text{-Bu}_4\text{N}]_5\text{Na}_3[(1,5\text{-COD})\text{Ir}\cdot\text{P}_2\text{W}_{15}\text{Nb}_3\text{O}_{62}]$ , **1**.

case, polyoxoanion-stabilized,  $\text{Ir}(0)_n$  metal colloid) [12d].

The methodology begins with: (i) the isolation of the active catalyst; (ii) proving that the isolated material is (or is not) still a kinetically competent catalyst (i.e., is as fast if not faster kinetically than the precatalyst); and (iii) using a variety of physical tools to characterize the isolated catalyst in-so-far as possible. (Example: the use of transmission electron microscopy (TEM) to provide evidence for, or against, the presence of classical Ir-oxide colloids “ $(\text{IrO}_2)_n$ ”).

### 3.2. Initial controls and catalytic activity studies

We began by first performing several necessary control experiments; then, we established the best conditions under which to isolate the most active form of the catalyst derived from  $[n\text{-Bu}_4\text{N}]_5\text{Na}_3[(1,5\text{-COD})\text{Ir}\cdot\text{P}_2\text{W}_{15}\text{Nb}_3\text{O}_{62}]$ , **1**. The control experiment in entry I in Table 1 shows that *without* added catalyst or ROOH initiator, only a background level (<4%) of cyclohexene conversion is seen, undoubtedly<sup>9</sup> due to trace ROOH impurities in even the purified cyclohexene, leading to autoxidation according to the Haber–Weiss pathway in Scheme 1. Entry II confirms this find-

ing by showing that with deliberately added ROOH (2-cyclohexen-1-yl hydroperoxide), but still without added catalyst, an average of ca. 9% cyclohexene conversion in 24 h<sup>10</sup> is seen. The three main non-peroxidic products [16], cyclohexene-1-one, cyclohexen-1-ol, and cyclohexene oxide are formed in ratios characteristic of allylic autoxidation via the Haber–Weiss, free-radical-chain mechanism [16,24a,b]. The third control experiment, entry III in Table 1, shows that the parent  $(n\text{-Bu}_4\text{N})_9\text{P}_2\text{W}_{15}\text{Nb}_3\text{O}_{62}$  polyoxoanion at the standard concentration, 1.26 mM, plus added ROOH initiator (20 mM)—but without  $\text{Ir}(\text{COD})^+$  present—gives no conversion above background (<3%). The fact that the conversion is below that of ROOH alone is not unexpected, and indicates the (redox) trapping of  $\text{ROO}^\bullet$  or other reaction intermediates by reaction with the  $\text{P}_2\text{W}_{15}\text{Nb}_3\text{O}_{62}^{9-}$  polyoxoanion [24a–c].

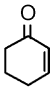
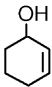
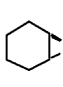
With the above controls in hand, our attention turned to the polyoxoanion-supported  $\text{Ir}^{\text{I}}$  catalyst,  $[n\text{-Bu}_4\text{N}]_5\text{Na}_3[(1,5\text{-COD})\text{Ir}\cdot\text{P}_2\text{W}_{15}\text{Nb}_3\text{O}_{62}]$ , **1**. Entry IV shows that the polyoxoanion-supported precatalyst, **1**, under the standard reaction conditions (i.e.,

<sup>9</sup> For lead reviews and references, see [24a–d]. For a state-of-the-art study, using a computer, numerical integration-modeled process with more than 74 reactions and leading to >100 products, see [24d].

<sup>10</sup> A control done as part of our earlier work on this reaction [16] showed that only negligible cyclohexen-1-ol and cyclohexen-1-one are formed due to the decomposition on the GC injector port of the 20 mM of added 2-cyclohexen-1-yl hydroperoxide initiator, ROOH. (However, at higher, 73 mM ROOH, some cyclohexen-1-ol and cyclohexen-1-one are seen [16].)

Table 1

Catalytic activity experiments, control experiments, and the effect of different precatalysts for cyclohexene oxidation in dichloromethane using molecular oxygen and 38 °C<sup>a</sup>

No.	Precatalyst	Conversion <sup>b</sup> (%)	Yield (%) <sup>c</sup>		
					
I	No catalyst; no ROOH initiator	4	2	1	1
II	No catalyst, but ROOH initiator was added	7	3	3	1
		12	6	4	2
		8	4	3	1
III	[ <i>n</i> -Bu <sub>4</sub> N] <sub>9</sub> P <sub>2</sub> W <sub>15</sub> Nb <sub>3</sub> O <sub>62</sub>	<3	–	–	–
IV	[ <i>n</i> -Bu <sub>4</sub> N] <sub>5</sub> Na <sub>3</sub> [(1,5-COD)Ir·P <sub>2</sub> W <sub>15</sub> Nb <sub>3</sub> O <sub>62</sub> ]	25	12	10	2
V	[ <i>n</i> -Bu <sub>4</sub> N] <sub>4</sub> Na <sub>2</sub> [(1,5-COD)Ir·SiW <sub>9</sub> Nb <sub>3</sub> O <sub>40</sub> ]	<3	–	–	–
VI	[(1,5-COD)IrCl] <sub>2</sub>	4	3	1	–
VII	[(1,5-COD)Ir(CH <sub>3</sub> CN) <sub>2</sub> ]BF <sub>4</sub>	8	4	3	1
VIII	[Ir <sub>2</sub> O(OH) <sub>2</sub> (1,5-COD) <sub>2</sub> Cl <sub>2</sub> ]	<3	–	–	–
IX	[(C <sub>8</sub> H <sub>12</sub> )Ir(CH <sub>3</sub> CN) <sub>2</sub> ]BF <sub>4</sub> /O <sub>2</sub> ; Sample A <sup>d</sup>	8	4	2	2
X	[(C <sub>8</sub> H <sub>12</sub> )Ir(CH <sub>3</sub> CN) <sub>2</sub> ]BF <sub>4</sub> /O <sub>2</sub> ; Sample B <sup>e</sup>	6	3	2	1
XI	[ <i>n</i> -Bu <sub>4</sub> N] <sub>2</sub> [(1,5-COD)Ir·P <sub>3</sub> O <sub>9</sub> ]	20	11	7	2
XII	[ <i>n</i> -Bu <sub>4</sub> N] <sub>2</sub> [(C <sub>8</sub> H <sub>11</sub> OH)Ir·P <sub>3</sub> O <sub>9</sub> ]	13	7	4	2
XIII	The precipitate from <b>1</b> <sup>f</sup>	12	6	4	2
XIV	The isolated catalyst from <b>1</b> <sup>g</sup>	23	12	9	2
		26	13	10	3
		9	5	4	–
XV	The O <sub>2</sub> -oxidized <b>1</b> as precatalyst <sup>h</sup>	12	6	5	1
XVI	The independently synthesized catalyst (using P <sub>2</sub> W <sub>15</sub> Nb <sub>3</sub> O <sub>62</sub> <sup>9-</sup> ) <sup>i</sup>	25	13	10	2
XVII	The independently synthesized catalyst (using P <sub>3</sub> O <sub>9</sub> <sup>3-</sup> ) <sup>i</sup>	18	10	7	1

<sup>a</sup> Reaction conditions: 6 ml CH<sub>2</sub>Cl<sub>2</sub>; 1.0 ml (9.87 mmol, 1.5 M) cyclohexene; catalyst (~1.26 mM; mol ratio catalyst/substrate ~1:1200); 1 atm dioxygen; 38 ± 0.1 °C; 24 h. In all experiments unless otherwise indicated, 0.14 mM 2-cyclohexen-1-yl hydroperoxide, ROOH initiator was also added.

<sup>b</sup> Conversion (%) is defined as [cyclohexene (mmol)]<sub>*t*=*t*</sub> / [cyclohexene (mmol)]<sub>*t*=0</sub> × 100%.

<sup>c</sup> Yield (%) is defined as [product (mmol)] / [cyclohexene (mmol)]<sub>*t*=0</sub> × 100%; products: cyclohexene oxide, cyclohexen-1-one and cyclohexen-1-ol.

<sup>d</sup> The solid was recovered from the *reaction solution* of the stoichiometric oxidation of [(1,5-COD)Ir(CH<sub>3</sub>CN)<sub>2</sub>]BF<sub>4</sub> (see Section 4.12) and redissolved without residue.

<sup>e</sup> The precipitate was recovered from the stoichiometric oxidation of [(1,5-COD)Ir(CH<sub>3</sub>CN)<sub>2</sub>]BF<sub>4</sub> (see Section 4.12) and remained insoluble during catalysis.

<sup>f</sup> The precipitate was recovered from a run under experimental conditions (see footnote a) using [*n*-Bu<sub>4</sub>N]<sub>5</sub>Na<sub>3</sub>[(1,5-COD)Ir·P<sub>2</sub>W<sub>15</sub>Nb<sub>3</sub>O<sub>62</sub>] as precatalyst (see Section 4.4). Most of the material remained insoluble during catalysis.

<sup>g</sup> The isolated catalyst was obtained as detailed in Section 4.4. The results in line 2 of this entry are from an independent experiment. In both cases the “isolated catalyst” was reused for catalysis immediately after its isolation. Line 3 shows the results obtained for the “isolated catalyst” sample used for the experiment in line 2, but after storage for 4 days (in the drybox, at room temperature).

<sup>h</sup> The oxidation product of the precatalyst **1** was prepared using standard reaction conditions (see footnote a) but *without* added cyclohexene (see Section 4.14) and was redissolved without residue.

<sup>i</sup> This material was prepared as detailed in Section 4.13.

1.26 mM catalyst, 20 mM ROOH initiator, 38 ± 0.1 °C, 1 atm O<sub>2</sub>, 24 h of reaction time) exhibits a conversion of cyclohexene of 25%, as high as seen for any of the 17 entries in Table 1. The three main, non-peroxidic products are again those proven elsewhere [16] to

be characteristic of the autoxidation of cyclohexene: cyclohexene-1-one, cyclohexen-1-ol, and cyclohexene oxide, entry IV (Table 1).

The results in entry V reveal that the catalytic activity of the (1,5-COD)Ir<sup>+</sup>-polyoxometalate-supported

Table 2

Summary of oxygen uptake results obtained for various catalyst precursors in the catalytic cyclohexene oxygenation with molecular oxygen<sup>a</sup>

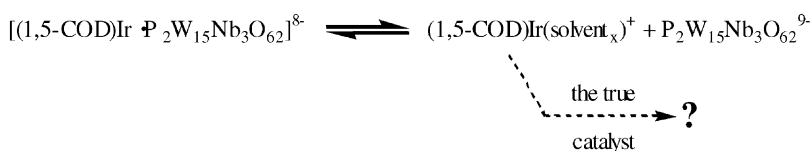
No.	Precatalyst (mmol)	O <sub>2</sub> -uptake (mmol)	Ratio [O <sub>2</sub> ]/[precatalyst]
I	[ <i>n</i> -Bu <sub>4</sub> N] <sub>5</sub> Na <sub>3</sub> [(1,5-COD)Ir·P <sub>2</sub> W <sub>15</sub> Nb <sub>3</sub> O <sub>62</sub> ] (0.37)	0.19	0.51
II	[ <i>n</i> -Bu <sub>4</sub> N] <sub>2</sub> [(1,5-COD)Ir·P <sub>3</sub> O <sub>9</sub> ] (0.52)	0.24	0.46
III	[(1,5-COD)IrCl] <sub>2</sub> (0.44)	0.58	1.32

<sup>a</sup> Reaction conditions: 1,2-dichloroethane or acetonitrile solvent, 10 ml; dioxygen, 1 atm; *T* = 273 K; 6–8 h of reaction time.

catalyst precursor depends upon the polyoxoanion type, an important result consistent with and supportive of a polyoxoanion-supported species as the true catalyst. The Keggin-type, SiW<sub>9</sub>Nb<sub>3</sub>O<sub>40</sub><sup>7-</sup> polyoxoanion complex, [*n*-Bu<sub>4</sub>N]<sub>4</sub>Na<sub>2</sub>[(1,5-COD)Ir·SiW<sub>9</sub>Nb<sub>3</sub>O<sub>40</sub>], is inferior to the Dawson, P<sub>2</sub>W<sub>15</sub>Nb<sub>3</sub>O<sub>62</sub><sup>9-</sup>-supported Ir<sup>I</sup> complex (cf. entries V–IV, Table 1). Note that it is known with certainty that the SiW<sub>9</sub>Nb<sub>3</sub>O<sub>40</sub><sup>7-</sup> polyoxoanion binds Ir<sup>I</sup> in a different, C<sub>s</sub> fashion [25] rather than the C<sub>3v</sub> symmetry fashion observed for the binding of Ir<sup>I</sup> in **1** (the symmetries cited reflect the support site of the underlying polyoxoanion) [11].

The next five entries, VI–X in Table 1 are for various *polyoxoanion-free* Ir<sup>I</sup> or their O<sub>2</sub>-oxidized Ir<sup>n+</sup> complexes. The results confirm that the polyoxoanion is necessary for the best catalyst. None of entries VI–X gave better than 8% cyclohexene conversion in 24 h, that is, none of the polyoxoanion-free Ir complexes show activity that is above the background activity of added ROOH alone over the same, 24 h (~9% conversion). The results in entries VI–X mirror previous investigations using of Vaska's complex, {[(C<sub>6</sub>H<sub>5</sub>)<sub>3</sub>P]<sub>2</sub>Ir<sup>I</sup>(CO)Cl}, which is catalytically active for cyclohexene autoxidation, but not in its dioxygen adduct (peroxidic), oxidized form {[(C<sub>6</sub>H<sub>5</sub>)<sub>3</sub>P]<sub>2</sub>Ir<sup>III</sup>O<sub>2</sub>(CO)Cl} [26].

Semi-quantitative kinetic evidence that **1**, and not free (1,5-COD)Ir(solvent)<sub>x</sub><sup>+</sup> formation, is responsible for the observed catalysis was obtained by adding free P<sub>2</sub>W<sub>15</sub>Nb<sub>3</sub>O<sub>62</sub><sup>9-</sup> to the original catalytic mixture to test the possibility of the following dissociative K<sub>eq</sub> to give free (1,5-COD)Ir(solvent)<sub>x</sub><sup>+</sup>:



When three equivalents of P<sub>2</sub>W<sub>15</sub>Nb<sub>3</sub>O<sub>62</sub><sup>9-</sup> were added to a CH<sub>2</sub>Cl<sub>2</sub> solution of **1** and cyclohexene, the normal catalytic reaction took place, with no detectable difference in the rate or conversion, results which rule out such a dissociative K<sub>eq</sub> in the catalytic autoxidation reaction. (Straightforward equilibrium calculations show that since K<sub>eq</sub> is ≪ 1 (we know this since all the observable (1,5-COD)Ir<sup>+</sup> is bound to the polyoxoanion [10a,c,11]), little to no catalytic activity would have been observed had this dissociative K<sub>eq</sub> been the predominant path to the active catalyst.)

We also determined O<sub>2</sub>-uptake stoichiometries for several of the compounds in Table 1; these results are reported in Table 2. Entry I in Table 2 reveals that 0.51 equiv. of O<sub>2</sub> are consumed by the Dawson, P<sub>2</sub>W<sub>15</sub>Nb<sub>3</sub>O<sub>62</sub><sup>9-</sup>-supported Ir<sup>I</sup> complex, indicating that 1.5 mol O<sub>2</sub> is used per mole of the Ir<sup>I</sup> complex. Entry II summarizes the results obtained for the analogous P<sub>3</sub>O<sub>9</sub><sup>3-</sup> complex, [(1,5-COD)Ir·P<sub>3</sub>O<sub>9</sub>]<sup>2-</sup>. Again, it is found that 1.5 mol O<sub>2</sub> is consumed by this complex. This result is consistent with the oxygen stoichiometry previously reported for this complex [21a], and provides further evidence for the quite similar catalytic behavior of [(1,5-COD)Ir·P<sub>3</sub>O<sub>9</sub>]<sup>2-</sup> and the Dawson polyoxometalate complex.

The oxygen uptake results for the dimeric [(1,5-COD)IrCl]<sub>2</sub> are shown in entry III. Approximately 1.32 equiv. of O<sub>2</sub> are consumed per mole of compound which is consistent with the expected—but different—1.5 mol O<sub>2</sub> required for the formation of [(1,5-COD)<sub>2</sub>Ir<sub>2</sub>O(OH)<sub>2</sub>Cl<sub>2</sub>] (Scheme 3) *vide supra*.



To summarize the results of the catalytic tests at this point, the best of the 12 entries in Table 1 discussed so far are those provided in entries IV and XI for, respectively, the polyoxoanion-supported  $[n\text{-Bu}_4\text{N}]_5\text{Na}_3[(1,5\text{-COD})\text{Ir-P}_2\text{W}_{15}\text{Nb}_3\text{O}_{62}]$  complex, and the trimetaphosphate-supported  $[n\text{-Bu}_4\text{N}]_2[(1,5\text{-COD})\text{Ir-P}_3\text{O}_9]$  complex. These semi-quantitative kinetic/catalytic results strongly suggest that the active species is indeed polyoxoanion-supported.

### 3.3. The evolution of the preferred, polyoxometalate-supported catalyst

With the above results in hand, a closer look at the evolution of the  $(n\text{-Bu}_4\text{N})_5\text{Na}_3[(1,5\text{-COD})\text{Ir-P}_2\text{W}_{15}\text{Nb}_3\text{O}_{62}]$ , **1**, complex into its active catalyst was undertaken. The time dependence of cyclohexene autoxidation in the presence of **1** is summarized in Fig. 2a, and a first-order ln plot of the cyclohexene loss data in Fig. 2b. Not apparent in Fig. 2a, but present, is a somewhat variable induction period (from less than one up to several hours) as seen in our earlier work and as fully expected for the Haber–Weiss radical-chain mechanism [16], even when ROOH initiator is deliberately added. Of greater significance to the present study, focused on whether or not the true catalyst is polyoxoanion-supported, is that, after 15–20 h (which corresponds to ca. 60–70 catalytic turnovers) the reaction mixture begins to turn cloudy due to the formation of a brownish precipitate, whereas the solution remains yellow. After 48 h (ca. 300 turnovers), the precipitate can account for up to ca. 30–50% by weight of the original sample of **1**, although the exact amount varies from run to run by up to ~30%, so that in some runs no visible precipitate was observed.

A key question which arises at this point is whether or not the precipitate is the active catalyst, so this point was investigated next. Note that, somewhat surprisingly, the formation of the precipitate does not affect quantitatively the shape of the cyclohexene loss vs. time curve, and does not result in a *detectably* non-linear first-order kinetic plot<sup>11</sup> (Fig. 2b), results

<sup>11</sup> The linearity of the kinetic plot in Fig. 2b and its inherent 10–15% error, along with the dependence of the autoxidation rate upon the  $[\text{catalyst}]^{1/2}$  demonstrated elsewhere [16], mean that up to ca. 35% of the precatalyst **1** can be converted into precipitate in the specific experiment shown in Fig. 2b (i.e., the  $[\text{catalyst}]$

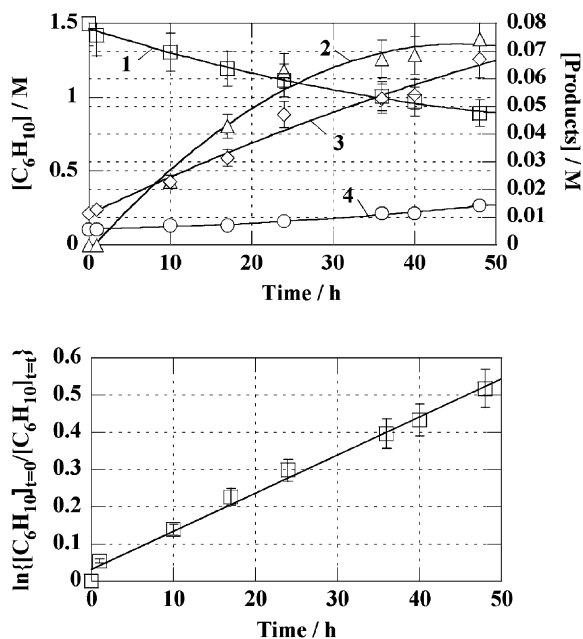


Fig. 2. (a) Time course of cyclohexene autoxidation in dichloromethane at 38 °C and 1 atm oxygen in the presence of the catalyst precursor  $[n\text{-Bu}_4\text{N}]_5\text{Na}_3[(1,5\text{-COD})\text{Ir-P}_2\text{W}_{15}\text{Nb}_3\text{O}_{62}]$ . Legend: cyclohexene, **1**; 2-cyclohexen-1-one, **2**; 2-cyclohexen-1-ol, **3**; cyclohexene oxide, **4**. (b) Pseudo-first-order plot of cyclohexene disappearance over a time range of 50 h. An initial rate of approximately  $11 \pm 1 \text{ h}^{-1}$  can be calculated from the slope of the first-order ln plot, normalized to the concentration of the catalyst (1.26 mM).

which suggest that the precipitate is not catalytically active, if only due to its insolubility in the reaction mixture. The control experiment in entry XIII (Table 1), confirms this prediction: the precipitate is *at most* ~50% as reactive as the precatalyst, **1**, barely more active than the background of added ROOH alone, without added catalyst of any type (cf. entries XIII, IV and II in Table 1).

can decrease by up to 35%), without detecting more than a ca. 15% change (due to the  $[\text{catalyst}]^{1/2}$  dependence) in the linearity of the ln plot (that ca. 15% change being within the maximum experimental error of the kinetic data)—in short, the ln plot in Fig. 2b is somewhat insensitive to changes in the  $[\text{catalyst}]$  simply due to the inherent form of the rate law.

### 3.4. Isolation of the catalyst and demonstration of the kinetic competence of the isolated material

The active catalyst was isolated from a cyclohexene oxidation experiment carried out under our standard cyclohexene oxidation conditions, but scaled up by a factor of 10 as detailed in Section 4.4. The isolated material, if reused immediately after its isolation, proved to be as active as any catalyst in Table 1 (see entries XIV, IV and XVI), exhibiting identical catalytic activity and selectivity within experimental error as the precatalyst  $[n\text{-Bu}_4\text{N}]_5\text{Na}_3[(1,5\text{-COD})\text{Ir}\cdot\text{P}_2\text{W}_{15}\text{Nb}_3\text{O}_{62}]$ , **1** (cf. entries XIV and IV, Table 1). Interestingly, a control experiment carried out 4 days after the actual catalyst isolation revealed a much lower activity, comparable to that observed without any catalyst, but with added ROOH initiator (i.e., Table 1, entry II). Even though the isolated catalyst was stored within the dry-box after its isolation, its activity deteriorates upon storage in the solid state. Another control experiment, entry XV in Table 1 shows that it is insufficient to just expose the precatalyst, **1**, to oxygen (i.e., without cyclohexene and ROOH initiator being present), as the resultant oxidized material is an inferior catalyst, one barely better than ROOH alone with no catalyst (entry II, Table 1).

With the active catalyst isolated, our attention turned to its characterization: Is it a colloidal material? Does it contain the parent  $\text{P}_2\text{W}_{15}\text{Nb}_3\text{O}_{62}^{9-}$  polyoxoanion, as required for a polyoxoanion-supported catalyst? If so, is the Ir to polyoxoanion ratio still 1:1? Note that, in the experiments below and since the catalyst solution and that solution evaporated to dryness (the isolated catalyst) appear to be one and the same material, those materials were used somewhat interchangeably in the experiments which follow.

### 3.5. TEM of the reaction solution and the precipitate

Since the cyclohexene oxidation reaction conditions used in this study (molecular oxygen as oxidant, with the formation of ROOH and  $\text{H}_2\text{O}$  during the oxidation reaction) could in principle lead to the formation of what the literature describes as blue, hydrous oxide type colloids “ $(\text{IrO}_2)_x\cdot(\text{H}_2\text{O})_y$ ” [27] (recall Scheme 5), TEM was used to analyze both a sample of the reaction solution, and the precipitate,

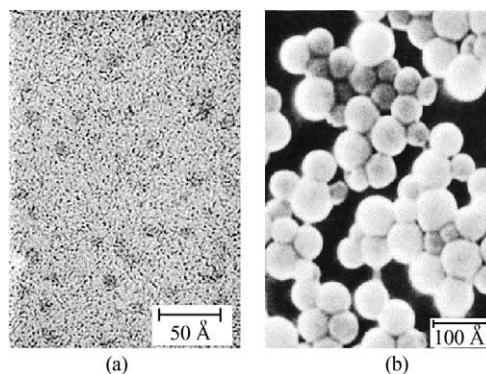


Fig. 3. Literature: (a) high resolution electron micrograph of  $\text{IrO}_2\cdot\text{H}_2\text{O}$  particles as produced by gamma radiolysis. (b) Scanning electron micrograph of aged  $\text{IrO}_2\cdot\text{H}_2\text{O}$  colloids produced by chemical methods (reprinted with permission [27]).

for the conceivable presence of such colloids. Note that although poorly compositionally characterized,<sup>12</sup> the “ $(\text{IrO}_2)_x\cdot(\text{H}_2\text{O})_y$ ” colloids are clearly visible by TEM, see Fig. 3 (reproduced from the literature [27]). Also note the dramatic effect of aging on the appearance of these particles, that is, their aggregation into much bigger spheres, about 1000 Å in diameter (Fig. 3b) after aging, a property of these colloids that we can compare to attempts to age our own catalyst.

Fig. 4a shows the TEM of a catalytically active solution recovered after 50 h (310 turnovers) of oxidation catalysis, with one drop of that solution deposited onto a carbon grid, dried and then analyzed by TEM. For a comparison, Fig. 4b shows also the micrograph of the pure iridium polyoxoanion, **1**, dissolved in dichloromethane then placed on a grid and analyzed by TEM that same day. The very close similarity between the particles in Fig. 4a and b, and the lack of any larger  $\text{Ir}_x$  particles (e.g., the sharp contrast with the size and the shape in comparison to the  $\text{Ir}(0)_{300}$  nanoclusters identified by TEM as reported elsewhere, for example [12c,d]) argue strongly for the absence of “ $(\text{IrO}_2)_n$ ” colloids. A rough estimate of  $\sim 15$  Å for the size of the (polyoxoanion) particles can be made, results which are in good agreement with the actual dimensions of the Dawson-type  $\text{P}_2\text{W}_{15}\text{Nb}_3\text{O}_{62}^{9-}$

<sup>12</sup> These literature colloids are presumably actually something closer to “ $\text{Ir}(\text{O})_x(\text{OH})_y(\text{Cl})_z^{n-}$ ”. They are formed by hydrolysis and reduction of hexachloroiridates; the extent of conversion depends upon different factors such as the nature of the oxidant and the pH of the solution [27].

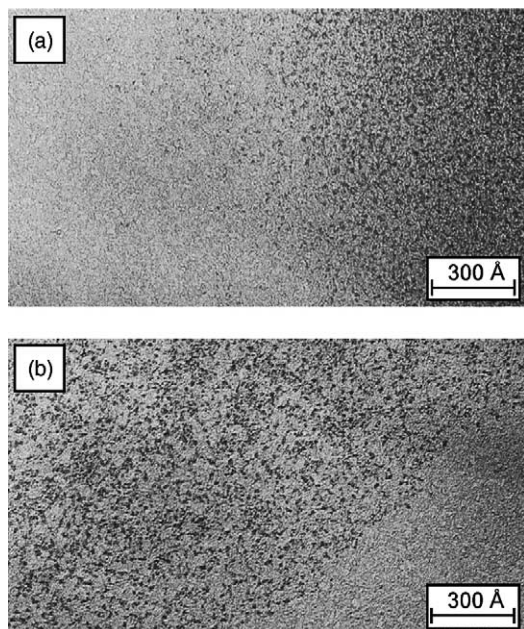


Fig. 4. (a) Transmission electron micrograph of the reaction solution of the catalytic cyclohexene autoxidation in the presence of  $[n\text{-Bu}_4\text{N}]_5\text{Na}_3[(1,5\text{-COD})\text{Ir}\cdot\text{P}_2\text{W}_{15}\text{Nb}_3\text{O}_{62}]$ , **1**. The sample for this TEM was taken from the same sample as that used for the ultracentrifugation MW measurements (entry III, Table 3). (b) The micrograph shows the TEM of solution of the catalyst precursor, **1**, in dichloromethane, done as a control experiment.

polyoxoanion of ca.  $12 \text{ \AA} \times 15 \text{ \AA}$ . In Fig. 5, the TEM image of the precipitate isolated from the solution and dissolved in acetonitrile is shown. Once again the micrograph in Fig. 5 is very similar to that of



Fig. 5. Transmission electron micrograph of the precipitate (see Section 4.4), recovered from the catalytic cyclohexene autoxidation reaction in the presence of the catalyst precursor  $[n\text{-Bu}_4\text{N}]_5\text{Na}_3[(1,5\text{-COD})\text{Ir}\cdot\text{P}_2\text{W}_{15}\text{Nb}_3\text{O}_{62}]$ , **1**, redissolved in acetonitrile and applied to a carbon-coated Cu TEM grid.

the pure polyoxoanion in Fig. 4b; the TEM in Fig. 5 rules out the presence of colloids or any other particles larger than ca.  $25\text{--}30 \text{ \AA}$ . Significantly, even after aging the solutions for several weeks the same micrographs as shown in Fig. 4a were obtained. This result especially in comparison to the dramatic size increase for authentic hydrous “ $(\text{IrO}_2)_x \cdot (\text{H}_2\text{O})_y$ ” colloids (Fig. 3b) as well as the difference in color of the two materials (the recovered polyoxoanion catalyst is yellow-orange while the literature “ $(\text{IrO}_2)_x \cdot (\text{H}_2\text{O})_y$ ” colloids are bluish), provides compelling evidence which rules out a traditional  $(\text{IrO}_2)_x \cdot (\text{H}_2\text{O})_y$ , non-polyoxoanion-stabilized<sup>13</sup> colloid.

### 3.6. Elemental analysis, IR and NMR results on the isolated catalyst

Given that TEM confirmed that the isolated catalyst is a discrete molecular species, and not a colloid, we turned to elemental analysis in order to establish the empirical formula of the isolated catalyst. The IR spectrum of the isolated catalyst (KBr pellet) clearly reveals that the  $\text{P}_2\text{W}_{15}\text{Nb}_3\text{O}_{62}^{9-}$  polyoxoanion is present, and structurally intact, by its characteristic absorptions in the polyoxometalate region ( $400\text{--}1200 \text{ cm}^{-1}$ ; listed in Section 4.4). Elemental analysis confirms that the 1:1 Ir to polyoxoanion ratio in the precatalyst **1**, is retained in the isolated catalyst (Ir:polyoxoanion ratio in the isolated catalyst = 1.1; see Section 4.4). In fact, for a non-crystalline, polyoxoanion complex, the elemental analysis is satisfactory for a formulation of the catalyst as “ $\{[(n\text{-Bu}_4\text{N})_6\text{Na}_3(\text{HO})_3\text{Ir}^{3+} \cdot \text{P}_2\text{W}_{15}\text{Nb}_3\text{O}_{62}]_x\}$ ”: (found) C, 19.68(20.06); H, 3.77(3.77); Ir, 3.28(3.64); N, 1.43(1.30); Na, 1.18(1.37); Nb, 4.76(4.95); P, 1.06(1.08); W, 47.08(45.16).

<sup>13</sup> It is important to note that the TEM results, alone, do not rule out the possibility of a completely new, hypothetical polyoxoanion-stabilized colloid something like “ $\text{Ir}_x\text{O}_y \cdot (\text{P}_2\text{W}_{15}\text{Nb}_3\text{O}_{62}^{9-})_z$ ” (recall Scheme 1, centermost part). However, the solution MW and other evidence which follows provided seemingly unequivocal evidence against this possibility as well. In addition, and while the  $\text{P}_2\text{W}_{15}\text{O}_{62}^{9-}$  polyoxoanion has been shown in other work to be an unusually effective stabilizing agent for electrophilic, coordinatively unsaturated  $\text{Ir}(0)_n$  colloidal metal surfaces [23,28], one may conclude that “ $\text{Ir}_x\text{O}_y$ ” colloids are probably really *anionic* “ $\text{Ir}_x\text{O}_y(\text{OH})_z^{n-}$ ” colloids, so that the *polyanionic* polyoxoanion would be repelled by, rather than attracted to (to thereby stabilize), these different type of hydroxy oxo-colloids.

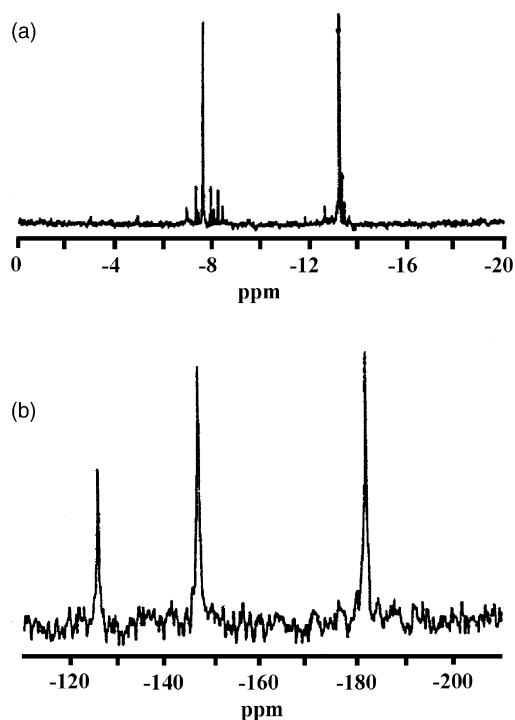


Fig. 6. (a)  $^{31}\text{P}$  NMR spectrum of the isolated catalyst (see Section 4.4) in  $\text{CD}_3\text{CN}$ . (b)  $^{183}\text{W}$  NMR spectrum of the isolated catalyst in  $\text{CD}_3\text{CN}$ . The observed three-line spectrum with relative intensities of 1:2:2 provides direct evidence for the presence of the  $\text{C}_{3v}$  symmetry,  $\text{P}_2\text{W}_{15}\text{Nb}_3\text{O}_{62}^{9-}$  polyoxoanion.

$^{31}\text{P}$  NMR spectroscopy (Fig. 6) (top spectrum), provides a second, direct demonstration that the isolated catalyst contains  $\text{P}_2\text{W}_{15}\text{Nb}_3\text{O}_{62}^{9-}$ , and that the polyoxoanion is intact. The  $^{31}\text{P}$  NMR further reveals that the isolated catalyst is ca. 85% one species by integration of the main, vs. the secondary,  $^{31}\text{P}$  peaks, and that the  $\text{Ir}^{n+}$  found by elemental analysis is almost surely supported on the polyoxoanion [this follows by a comparison of the chemical shifts observed ( $\delta$   $-6.8$ ,  $-13.7$  ppm in  $\text{CD}_3\text{CN}$ ) to those for the free  $\text{P}_2\text{W}_{15}\text{Nb}_3\text{O}_{62}^{9-}$  ( $\delta$   $-6.3$  ( $\pm 0.4$ ),  $-13.5$  ( $\pm 0.4$ ) ppm in  $\text{CD}_3\text{CN}$ )]. Note that the  $\delta$   $-6.8$   $^{31}\text{P}$  resonance in the isolated complex is the one closest to the  $[\text{Nb}_3\text{O}_9]^{3-}$  support site (“north end”; recall Fig. 1) of the  $\text{P}_2\text{W}_{15}\text{Nb}_3\text{O}_{62}^{9-}$  and its downfield chemical shift vs. that of the parent  $\text{P}_2\text{W}_{15}\text{Nb}_3\text{O}_{62}^{9-}$  is strong evidence (based on our earlier work on supported complexes [5,10]) that the  $\text{Ir}^{n+}$  found by elemental

analysis is supported on the polar,  $[\text{Nb}_3\text{O}_9]^{3-}$  support-site of the polyoxoanion.

The primarily three-line  $^{183}\text{W}$  NMR (Fig. 6) (bottom spectrum) confirms the  $^{31}\text{P}$  NMR by showing: (i) that intact  $\text{P}_2\text{W}_{15}\text{Nb}_3\text{O}_{62}^{9-}$  is clearly present; (ii) that the isolated catalyst sample is primarily one species (although, in our experience, lower levels of other species are readily missed by the relatively insensitive  $^{183}\text{W}$  NMR); (iii) that the major species present appears to be of  $\text{C}_{3v}$  symmetry—the most common symmetry we have observed for  $\text{P}_2\text{W}_{15}\text{Nb}_3\text{O}_{62}^{9-}$ -supported organometallics [5,10,11]. Note that the  $^{183}\text{W}$  and  $^{31}\text{P}$  NMR, plus the IR and elemental analysis, are *definitive in showing that  $\text{Ir}^{n+}$  plus the  $\text{P}_2\text{W}_{15}\text{Nb}_3\text{O}_{62}^{9-}$  polyoxoanion in a 1:1 ratio are part of the isolated, active and preferred catalyst.*

We also attempted to investigate the fate of the 1,5-COD ligand present in the precatalyst **1** by GC,  $^1\text{H}$  NMR and  $^{13}\text{C}$  NMR. However, we failed to see any signals expected for the 1,5-COD ligand or its oxygenation products (for details see Section 4.4); only the signals expected for the  $n\text{-Bu}_4\text{N}^+$  cations in the catalyst precursor, as well as in the isolated catalyst, could be detected. This is also in agreement with the results of the elemental analysis obtained for the isolated catalyst (see Section 4.4), which provided no evidence for the presence of C or H from sources other than the  $n\text{-Bu}_4\text{N}^+$  cations. It seems possible at this point that the COD ligand has been displaced during the transformation of **1** into the active catalyst. Overall, the elemental analysis plus spectroscopic studies establish an *approximate* formula for the active catalyst as “[ $(n\text{-Bu}_4\text{N})_6\text{Na}_3(\text{HO})_3\text{Ir}^{3+}\cdot\text{P}_2\text{W}_{15}\text{Nb}_3\text{O}_{62}$ ] $_x$ ”.

### 3.7. Crystallization trials with the isolated catalyst

Given that the NMR studies suggested that primarily one species was present in the isolated catalyst, we tried to crystallize the isolated catalyst from a combination of  $\text{CH}_3\text{CN}$ ,  $\text{CH}_2\text{Cl}_2$ , and  $\text{ClCH}_2\text{CH}_2\text{Cl}$ . Unfortunately no crystalline material suitable for X-ray crystallography was ever obtained. This result, although unfortunate, is not unexpected given the solution molecular weight studies which follow and which indicate the presence of  $\geq 2$  species in solution.

### 3.8. Solution molecular weight experiments by analytical ultracentrifugation

Our efforts turned next to solution molecular measurements in CH<sub>3</sub>CN. These were used to determine the molecular weight of the principle species present in the catalyst solution, in the isolated catalyst, and in the precipitate that forms from the catalytically active solution. First, the solution molecular weight [n-Bu<sub>4</sub>N]<sub>9</sub>P<sub>2</sub>W<sub>15</sub>Nb<sub>3</sub>O<sub>62</sub> was determined as a control experiment. The [n-Bu<sub>4</sub>N]<sub>9</sub>P<sub>2</sub>W<sub>15</sub>Nb<sub>3</sub>O<sub>62</sub> was synthesized under conditions that avoid formation of the Nb–O–Nb bridged anhydride [7a],<sup>14</sup> so that a “monomeric” weight in the sedimentation-equilibrium experiment was expected. Indeed, at rotor speeds of 20,000 and 30,000 rpm the experimentally determined solution molecular weight of [n-Bu<sub>4</sub>N]<sub>9</sub>P<sub>2</sub>W<sub>15</sub>Nb<sub>3</sub>O<sub>62</sub> ranged from 5500 (±300) g/mol to 5700 (±300) g/mol. These values suggest that the sedimenting species is somewhere between [(n-Bu<sub>4</sub>N)<sub>5</sub>P<sub>2</sub>W<sub>15</sub>Nb<sub>3</sub>O<sub>62</sub>]<sup>4-</sup> (for which the calculated molecular weight is 5303 g/mol) and [(n-Bu<sub>4</sub>N)<sub>8</sub>P<sub>2</sub>W<sub>15</sub>Nb<sub>3</sub>O<sub>62</sub>]<sup>1-</sup> (for which the calculated molecular weight is 6030 g/mol). The extent of n-Bu<sub>4</sub>N<sup>+</sup> ion-pairing observed here is consistent with past results on similar systems [6a,b,e]. The data for the experiment run at 20,000 and 30,000 rpm are well-fit by an ideal, single-species model, as indicated by the random distribution of residuals about the 0.0 line. Also worth noting is that the solution molecular weight of [n-Bu<sub>4</sub>N]<sub>9</sub>P<sub>2</sub>W<sub>15</sub>Nb<sub>3</sub>O<sub>62</sub> was determined under conditions as identical as possible to those used for the isolated catalyst.

For the *catalytic solution* after 50 h of reaction time (the identical solution from which a sample for the TEM in Fig. 4a was taken), a species with a molecular weight of approximately 6000 (±500) a.m.u. was observed, indicating the presence of the P<sub>2</sub>W<sub>15</sub>Nb<sub>3</sub>O<sub>62</sub><sup>9-</sup> polyoxoanion and the Ir<sup>n+</sup> in a *monomeric form* in the catalyst solution. Interestingly, the *precipitated material* shows a molecular weight of ca. 10500, indicating that the precipitate is a non-colloidal, molecular, *but dimer-like aggregate*.

These molecular weight results confirm the TEM studies by ruling out a colloidal, or any another, more highly aggregated form,<sup>15</sup> for both the catalyst and the precipitate, at least under the stated conditions of the MW measurements and in CH<sub>3</sub>CN, a statement that is fortified by the fact that Edlund [28], and Vargaftik et al. [29], have been able to detect intact nano-colloids by ultracentrifugation molecular measurements.

The solution molecular weight studies on the isolated catalyst proved more complicated, but interesting. At rotor speeds of 20,000 and 30,000 rpm two separate experimentally determined solution molecular weights of the same sample of the isolated catalyst gave 10,900 (±500) g/mol (approximately the expected molecular weight of a “dimer”) and 7900 (±400) g/mol, respectively. These two values are obviously not within experimental error of each other. It was found that there are obvious systematic deviations from the 0.0 line in the residuals of both experiments. These deviations from the 0.0 line in the residuals clearly indicate that an ideal, single-species model for the *isolated catalyst* ultracentrifugation data is not correct [30a–d]. One explanation is that the sample is “heterogeneous”, that is, the sample contains a mixture of non-interconverting species. For example, a mixture of non-interconverting species containing mostly the “dimeric” form of the catalyst, but also containing some monomeric form, could account for these results.<sup>16</sup> This means that the “average” molecular weight obtained is not necessarily a true average because the heavier species in solution have a greater tendency to sediment out of the measurable

<sup>15</sup> No heavier precipitate was seen in the bottom of the centrifugation cell; that is, we took care to ensure that ultracentrifugation rotation speed was in fact appropriate for the molecular weight of the predominant species in solution.

<sup>16</sup> A second possibility is that some self-association phenomenon like hydrogen bonding is occurring. A third possibility is that the sample is behaving in a non-ideal manner. A fourth possibility is that some combination of these phenomena is occurring. The second and third possibilities, and therefore the fourth possibility as well, seem unlikely for the following reasons. A self-association phenomenon (like hydrogen bonding) is unprecedented for these compounds. Also, it is not clear why the isolated catalyst would self-associate when [n-Bu<sub>4</sub>N]<sub>9</sub>P<sub>2</sub>W<sub>15</sub>Nb<sub>3</sub>O<sub>62</sub> does not self-associate under very similar conditions. The same argument can be made for the possibility of non-ideality. Why would the isolated catalyst behave non-ideally when [n-Bu<sub>4</sub>N]<sub>9</sub>P<sub>2</sub>W<sub>15</sub>Nb<sub>3</sub>O<sub>62</sub> does not behave non-ideally under very similar conditions?

<sup>14</sup> Note the two typographical errors in this paper: p. 7910, right-hand column, 12th line: “84% excess” should read “2% excess” and p. 7910, footnote 20, 4th line: “5%” should read “0.5”.

concentration gradient at higher rotation speeds. This is in perfect agreement with the data for the *isolated catalyst*—the higher rotor speed (30,000 rpm vs. 20,000 rpm) gave a smaller average weight (7900 ( $\pm 400$ ) g/mol vs. 10,900 ( $\pm 500$ ) g/mol, respectively). By the same argument, the lower rotor speed gives a better estimate of the true average molecular weight.

Assuming that the preceding interpretation of the data for the isolated catalyst is correct, then one can conclude that the investigated *isolated catalyst* is in a dimeric (possibly  $\mu$ -OH or  $\mu$ -O-bridged) form that is catalytically less active than the precatalyst **1**. Note that, due to the experimental requirements for the solution molecular weight determination, this experiment could not be done using the freshly isolated, *active* catalyst. It seems possible—but unproven—then, that the formation of a dimeric species is associated with the observed loss in activity, and that monomeric form maybe the active form of the catalyst derived from **1**.

### 3.9. Mass spectroscopy

The positive ion fast atom bombardment mass spectrometry (FAB-MS) [31] for the isolated catalyst is shown in Fig. 7a. The spectrum appears to be analogous to that of the parent polyoxoanion  $P_2W_{15}Nb_3O_{62}^{9-}$  (Fig. 7b) with main peaks in the 5500–6200 a.m.u. as seen and assigned elsewhere [30].

In Fig. 8a, the positive ion spectrum of the catalyst precursor **1** is shown. The spectrum seen is analogous to that seen and assigned before (Fig. 2 elsewhere [30]), with main peaks in the 5500–6200 a.m.u. range due to the  $P_2W_{15}Nb_3O_{62}^{9-}$  polyoxoanion (e.g.,  $[H(n-Bu_4)_9P_2W_{15}Nb_3O_{62}]^+$  at 6273 [30]). Also seen is a bit of a Nb–O–Nb bridged, polyoxoanion anhydride peak between 10,000 and 11,000, results which show that it is difficult to distinguish unequivocally monomers vs. dimers of at least this type of polyoxoanion by FAB-MS, a conclusion also reached in earlier work [30].

The positive ion FAB-MS for the precipitate is shown in Fig. 8b; the presence of a much stronger dimer peak at ca. 10,300 is consistent with the solution MW measurement, although an even stronger, broad peak centered near 5500 means, rigorously, that either the dimer decomposes under the FAB-MS con-

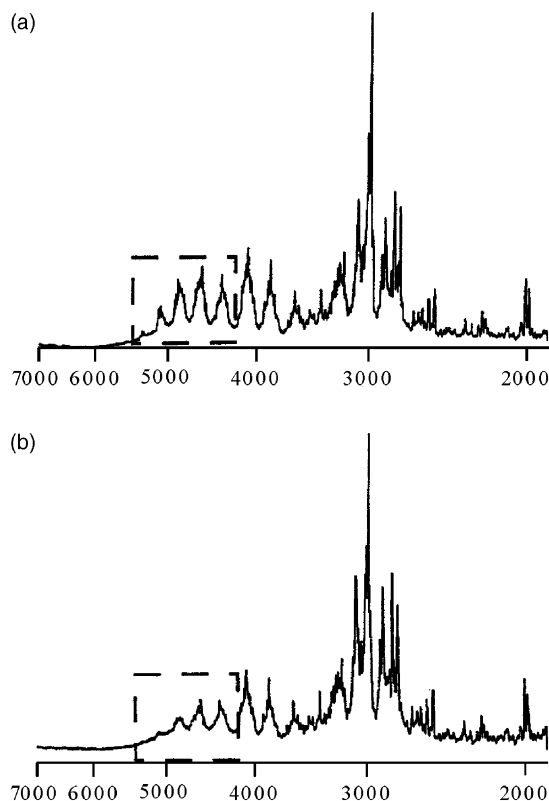


Fig. 7. (a) Positive FAB-MS spectrum of the isolated catalyst. The positive FAB-MS spectrum of the parent  $[n-Bu_4N]_9P_2W_{15}Nb_3O_{62}$  polyoxometalate (b) is provided for comparison. The spectra are almost superimposable, confirming the presence of  $P_2W_{15}Nb_3O_{62}^{9-}$  in the isolated catalyst.

ditions to a monomer, or that the monomer is the true species and the dimer has formed under the FAB-MS conditions.

In short, the FAB-MS results: (i) confirm that the polyoxoanion is part of the active catalyst and the precipitate; and (ii) provide additional evidence that the precipitate is in an aggregated, dimeric form.

### 3.10. Ion-exchange resin experiments for inner-sphere $Ir^{n+}$ to polyoxoanion bonding

A final piece of evidence that the isolated catalyst contains covalent, inner-sphere bonding of oxidized  $Ir^{n+}$  to the  $P_2W_{15}Nb_3O_{62}^{9-}$  polyoxoanion was obtained from experiments employing ion-exchange resins. As detailed in Section 4.10, in separate

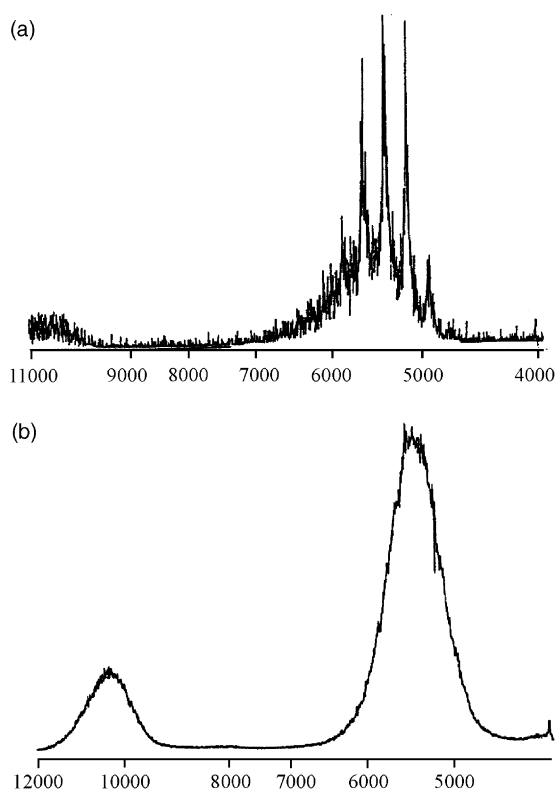


Fig. 8. (a) Positive FAB-MS spectra of the catalyst precursor (top), and the precipitate (b), recovered from the catalytic cyclohexene autoxidation in the presence of the catalyst precursor  $[n\text{-Bu}_4\text{N}]_5\text{Na}_3[(1,5\text{-COD})\text{Ir}\cdot\text{P}_2\text{W}_{15}\text{Nb}_3\text{O}_{62}]$ , **1**.

experiments acetonitrile solutions of first the precatalyst **1**, and then the isolated catalyst, *vide supra* were loaded onto a *cation*-exchange column in the  $n\text{-Bu}_4\text{N}^+$  form,  $\text{P}\text{-SO}_3^-\text{-}n\text{-Bu}_4\text{N}^+$  (P: macroreticular polymer), and then slowly eluted down the column with  $\text{CH}_3\text{CN}$ . No retention of the yellow-brown *anionic* precatalyst **1** was observed as expected; the same result was found when the experiment was repeated using a sample of the isolated catalyst. In a second series of experiments, precatalyst **1**, and then separately a sample of the isolated catalyst, were loaded onto separate *anion*-exchange columns in their  $\text{Cl}^-$  form,  $\text{P}\text{-NR}_3^+\text{Cl}^-$  (P: macroreticular polymer). In both experiments the colored, anionic complexes were completely retained on the column. These results are completely consistent with our recent, analogous findings on the non-ion-exchangeability

of polyoxoanion-supported  $\text{Mn}^{n+}$  complexes that are catalysts for cyclohexene and norbornene oxygenations using  $[\text{PhIO}]_n$  [14]. As part of the present work we also performed two separate control experiments (carried out under Ar) in which a solution of  $[(1,5\text{-COD})\text{Ir}(\text{CH}_3\text{CN})_2]\text{BF}_4$  in acetonitrile was loaded onto the same cation- and anion-exchange columns. As expected for these controls, the cationic  $[(1,5\text{-COD})\text{Ir}(\text{CH}_3\text{CN})_2]^+$  complex is retained on the  $\text{P}\text{-SO}_3^-\text{-}n\text{-Bu}_4\text{N}^+$  cation-exchange column but passes through the  $\text{P}\text{-NR}_3^+\text{Cl}^-$  anion-exchange column.

In summary, even by themselves, the ion-exchange experiments confirm the inner-sphere bonding of  $[(1,5\text{-COD})\text{Ir}(\text{I})]^+$  to  $\text{P}_2\text{W}_{15}\text{Nb}_3\text{O}_{62}^{9-}$  in the precatalyst, **1** (a bonding directly demonstrated previously by  $^{17}\text{O}$  NMR [11]), and provide good evidence for  $\text{Ir}^{n+}$  to  $\text{P}_2\text{W}_{15}\text{Nb}_3\text{O}_{62}^{9-}$  bonding in the isolated catalyst as well. At this point there is a clear answer to the title question of “Is the true catalyst polyoxoanion-supported or not?”. *It is supported.*

### 3.11. Initial development of an independent synthesis to an active $\text{P}_2\text{W}_{15}\text{Nb}_3\text{O}_{62}^{9-}$ -supported $\text{Ir}^{n+}$ catalyst

Since the application of virtually all applicable physical methods failed to provide the exact structure for the active catalyst, and in the absence of strongly diffracting single crystals, we took the one remaining approach that we could conceive of to better identify the catalyst’s structure: we attempted an independent synthesis of the active catalyst.

Entry XVI in Table 1 shows that by combining the product from the *preoxidation* of the iridium precursor  $[(1,5\text{-COD})\text{Ir}(\text{CH}_3\text{CN})_2]\text{BF}_4$  with  $[n\text{-Bu}_4\text{N}]_9\text{P}_2\text{W}_{15}\text{Nb}_3\text{O}_{62}$  (see Section 4.13), we have been able to *independently synthesize* a cyclohexene autoxidation catalyst that is identically as active (25% cyclohexene conversion in 24 h, see Table 1) as either of the other two, most active entries in Table 1 (i.e., starting with the precatalyst **1**, entry IV, or using the isolated catalyst, entry XIV). Infrared measurements on what we will call the “synthesized catalyst” confirm the presence of a Dawson-type  $\text{P}_2\text{W}_{15}\text{Nb}_3\text{O}_{62}^{9-}$  heteropolytungstate framework; a  $^{31}\text{P}$  NMR spectrum of this material in  $\text{CD}_3\text{CN}$  shows two lines at  $\delta -7.2$  and  $-13.3$  ppm with integrated intensities of 1:1 compared to  $\delta = -6.8$  and  $-13.7$  ppm for the

isolated catalyst in CD<sub>3</sub>CN. (Note the error bars on these shifts are typically not better than  $\pm 0.4$  for the reasons detailed in footnote 18 elsewhere [6j].) Of note is that the <sup>31</sup>P resonance observed for the “north” <sup>31</sup>P atom located directly beneath the [Nb<sub>3</sub>O<sub>9</sub>]<sup>3-</sup> cap (recall the polyoxoanion’s structure back in Fig. 1) is broadened and reduced in its height, direct evidence for a support interaction between the polyoxoanion and the [(1,5-COD)Ir(CH<sub>3</sub>CN)<sub>2</sub>]BF<sub>4</sub>/O<sub>2</sub> oxidation product. The <sup>183</sup>W NMR spectrum of the synthesized catalyst exhibits three resonances with integrated intensities for the three peaks of 1:2:2 as expected for the presence of a largely C<sub>3v</sub> (average; pseudo [10a]) symmetry Ir<sup>n+</sup> polyoxoanion complex.

The two most important points here are that: (i) the evidence again clearly points to the presence of a polyoxoanion-supported, Ir<sup>n+</sup> catalyst; and (ii) a new, simplified approach to characterizing the oxidized Ir<sup>n+</sup> species of an active catalyst has been unveiled. Specifically, one should now be able to characterize the much smaller, and thus presumably more tractable, [(1,5-COD)Ir(CH<sub>3</sub>CN)<sub>2</sub>]BF<sub>4</sub>/O<sub>2</sub> oxidation product *before* it is added to the parent P<sub>2</sub>W<sub>15</sub>Nb<sub>3</sub>O<sub>62</sub><sup>9-</sup> polyoxoanion to yield what we have shown is an active catalyst. We do not, however, have plans to pursue this, our own interests and funding haven taken a different path, namely towards novel polyoxoanion-stabilized nanocluster catalysts [12c,d].

### 3.12. Summary and conclusions

The main question posed in this paper is, when starting with [*n*-Bu<sub>4</sub>N]<sub>5</sub>Na<sub>3</sub>[(1,5-COD)Ir·P<sub>2</sub>W<sub>15</sub>Nb<sub>3</sub>O<sub>62</sub>], **1**, as the precatalyst for the autoxidation of cyclohexene, “Is the resultant, true catalyst polyoxoanion-supported?”. The data obtained are compelling in indicating that the active catalyst indeed involves a P<sub>2</sub>W<sub>15</sub>Nb<sub>3</sub>O<sub>62</sub><sup>9-</sup> polyoxoanion-supported Ir<sup>n+</sup> complex in a 1:1, monomeric form. The evidence comes: (i) from kinetics, since the presence of the polyoxoanion increases the autoxidation rate 100-fold in the absence of ROOH initiation [13] and still ~3-fold in the presence of a sizable amount of ROOH initiator, entries IV and II in Table 1, and since all forms of Ir<sup>n+</sup> tested in the absence of the polyoxoanion, Table 2 shows little reactivity above background; (ii) from elemental analysis and spectroscopic evidence

(IR, and <sup>31</sup>P and <sup>183</sup>W NMR) which indicate the presence, in a ~1:1 ratio, of both the polyoxoanion and the oxidized Ir<sup>n+</sup>; (iii) from MW measurements (ultracentrifugation and FAB-MS) which confirm the presence of the polyoxoanion; (iv) from <sup>31</sup>P NMR and ion-exchange resin evidence that the Ir<sup>n+</sup> is bonded to the [Nb<sub>3</sub>O<sub>9</sub>]<sup>3-</sup> support site in the P<sub>2</sub>W<sub>15</sub>Nb<sub>3</sub>O<sub>62</sub><sup>9-</sup> polyoxoanion.

In short, the results answer the title question “Is the true catalyst polyoxoanion-supported?” with “yes”, and reveal a working, average formula for the catalyst as “[(*n*-Bu<sub>4</sub>N)<sub>6</sub>Na<sub>3</sub>(HO)<sub>3</sub>Ir<sup>3+</sup>·P<sub>2</sub>W<sub>15</sub>Nb<sub>3</sub>O<sub>62</sub>]<sub>x</sub>” (*x* = 1, 2). The answer is significant, even if the (auto)oxidation reaction catalyzed is not, as the historically first example [13] of a polyoxoanion-supported catalyst in that polyoxoanion-supported catalysts are one of the eight new subclasses of polyoxoanions in catalysis [14].

The second example has been reported recently, [(CH<sub>3</sub>CN)<sub>x</sub>Mn<sup>n+</sup>·P<sub>2</sub>W<sub>15</sub>Nb<sub>3</sub>O<sub>62</sub><sup>9-</sup>]<sup>n-9</sup> oxidation catalysts for cyclohexene and norbornene oxygenation using [PhIO]<sub>n</sub> as the oxidant [14]. A potential third example which employs the Fe(II) plus vanadium polyoxoanion complexes [(CH<sub>3</sub>CN)<sub>x</sub>Fe·P<sub>2</sub>W<sub>15</sub>V<sub>3</sub>O<sub>62</sub>]<sup>7-</sup> and [(CH<sub>3</sub>CN)<sub>x</sub>Fe·SiW<sub>9</sub>V<sub>3</sub>O<sub>40</sub>]<sup>5-</sup> serving as *pre-catalysts* for a record, >100,000 total turnovers, of catechol dioxygenase catalysis using molecular oxygen has also been reported [32]. However, the mechanistic work to date suggests that the true catalyst does not involve the intact polyoxoanion or even require Fe<sup>n+</sup>—only V appears to be essential.

What is perhaps most telling from this study is the level of effort required to develop new subclasses of polyoxoanion-based catalysts, that is, to synthesize, test for catalytic activity, and then especially to do the necessary kinetic and mechanistic studies to establish the true identity of the catalyst. In the present case the studies have proceeded off and on over more than a decade; in the work leading to novel polyoxoanion-stabilized nanoclusters, more than a half-decade for the mechanistic work alone [12d] was required [12c]. Even when combined, these studies only set the conceptual stage for the possible discovery of practical applications of these, and the other seven, new classes of polyoxoanion-based catalysts shown in Fig. 1 elsewhere [14]. Those efforts will probably require combinatorial-type survey studies.



## 4. Experimental

### 4.1. Materials

All commercially obtained compounds were Baker reagent grade unless otherwise noted. The following reagents were obtained from Aldrich and were used as received: 4,7,13,16,21,24-hexaoxa-1,10-diazabicyclo [8.8.8]hexacosane [Kryptofix<sup>®</sup> 2.2.2.] (used to remove Na<sup>+</sup> ion-pairing effects from polyoxoanion NMRs, *vide infra*), anhydrous Et<sub>2</sub>O (HPLC grade), CH<sub>3</sub>CN (HPLC grade), EtOAc (HPLC grade). [(1,5-COD)IrCl]<sub>2</sub> was obtained from stream and used as received. Deuterated NMR solvents (CD<sub>3</sub>CN, CDCl<sub>3</sub>; Cambridge Isotope Laboratories) were used as received. When NMR samples are stated as being prepared in the drybox, the deuterated solvent was degassed by either purging with the drybox atmosphere or, if degassed outside the drybox, by purging with argon for 0.5 h before bringing the degassed solvent into the drybox. The heteropolyoxoanion-supported complex [n-Bu<sub>4</sub>N]<sub>5</sub>Na<sub>3</sub>[(1,5-COD)Ir·P<sub>2</sub>W<sub>15</sub>Nb<sub>3</sub>O<sub>62</sub>], **1**, was prepared and characterized according to our previously reported, improved procedure [7a] (see also [10]). [Ir<sub>2</sub>O(OH)<sub>2</sub>(1,5-COD)<sub>2</sub>Cl<sub>2</sub>] was prepared by reaction of [Ir(1,5-COD)Cl]<sub>2</sub> with molecular oxygen in dichloromethane following a procedure described elsewhere [20b]; the product was characterized by IR spectroscopy in comparison to the literature [20b] (IR, KBr pellet, cm<sup>-1</sup>; 1490(s), 1418(s), 1328(m), 1302(m), 1228(w), 1178(w), 1088(w), 1005(m), 902(m), 885(m), 848(s), 798(m), 695(vs), 610(w), 595(w), 535(w), 485(vs)). [n-Bu<sub>4</sub>N]<sub>2</sub>[(1,5-COD)Ir·P<sub>3</sub>O<sub>9</sub>] and [n-Bu<sub>4</sub>N]<sub>2</sub>[(C<sub>8</sub>H<sub>11</sub>OH)Ir·P<sub>3</sub>O<sub>9</sub>] were prepared as reported previously [21], and characterized by <sup>13</sup>C and <sup>31</sup>P NMR in comparison to the literature [21]. [n-Bu<sub>4</sub>N]<sub>2</sub>[(1,5-COD)Ir·P<sub>3</sub>O<sub>9</sub>]; <sup>13</sup>C{<sup>1</sup>H} NMR (75.5 MHz, CD<sub>3</sub>CN, 20 °C, 0.15 M): δ 65.3, 31.9. <sup>31</sup>P NMR (121.5 MHz, CD<sub>3</sub>CN, 20 °C, 0.15 M): δ -11.6(s). (n-Bu<sub>4</sub>N)<sub>2</sub>[(C<sub>8</sub>H<sub>11</sub>OH)Ir·P<sub>3</sub>O<sub>9</sub>]; <sup>13</sup>C{<sup>1</sup>H} NMR (75.5 MHz, CD<sub>3</sub>CN, 20 °C, 0.07 M): δ 87.8, 74.7, 44.9, 44.8, 39.4, 37.9, 31.8, 27.2. <sup>31</sup>P NMR (121.5 MHz, CDCl<sub>3</sub>, 20 °C, 0.04 M): δ -1.1(dd), -3.3(dd), -8.4(dd). 2-Cyclohexen-1-yl hydroperoxide was prepared, and the amount of active peroxide determined by iodometric titration, as described elsewhere [16]; additional literature on 2-cyclohexen-1-yl hydroperoxide is available as well [33].

### 4.2. Instrumentation/analytical procedures

Air-sensitive samples were prepared in a vacuum atmospheres inert atmosphere glove box (<1 ppm O<sub>2</sub> concentration). The UV spectra were recorded using a HP 8452A diode array system interfaced to an IBM 486 computer. Infrared spectra were obtained on a Nicolet 5DX spectrometer as KBr disks. KBr (Aldrich, spectrophotometric grade) was used as received. The NMR spectra of routine samples were obtained as CDCl<sub>3</sub> or CD<sub>3</sub>CN solutions in Spectra Tech or Wilmad NMR tubes. Air-sensitive samples were prepared in the drybox, and the solution was placed in an NMR tube (5 mm o.d.) equipped with a J. Young airtight valve (Wilmad), at room temperature unless otherwise stated. The chemical shifts are reported on the scale with downfield resonances as positive. <sup>183</sup>W NMR spectra were collected on a Bruker AM500 NMR spectrometer using 10 mm o.d. NMR tubes. The <sup>183</sup>W NMR spectra were referenced externally by the substitution method to 2 M Na<sub>2</sub>WO<sub>4</sub>/D<sub>2</sub>O (pD 8.0). Spectral parameters for <sup>183</sup>W (20.838 MHz) include: pulse width 30 ms; acquisition time 1114 ms; sweep width ±14705 Hz. A 10 Hz exponential apodization of the FID was used on all spectra, but was removed for any linewidths reported herein. <sup>31</sup>P NMR (121.5 MHz) spectra were recorded in 5 mm o.d. tubes on a Bruker AC-300P NMR spectrometer. A 33 mM CD<sub>3</sub>CN solution (0.020 mmol of polyoxoanion in 0.6 ml) was used unless otherwise stated. An external reference of 85% H<sub>3</sub>PO<sub>4</sub> was used by the substitution method. Acquisition parameters are as follows: <sup>31</sup>P tip angle 45° (pulse width 5 μs); acquisition time, 1.436 s; relaxation delay, 1.000 s; and sweep width, 10000 Hz. An exponential line broadening apodization (2.0 Hz) was applied to all spectra, but removed for any linewidths reported. <sup>1</sup>H NMR (300.15 MHz) and <sup>13</sup>C NMR (75.0 MHz) spectra were recorded in 5 mm o.d. tubes on a Bruker AC-300 NMR spectrometer, at 21 °C unless otherwise noted, and were referenced to the residual impurity in the deuterated solvent (<sup>1</sup>H NMR) or to the deuterated solvent itself (<sup>13</sup>C NMR). Spectral parameters for <sup>1</sup>H NMR: <sup>1</sup>H tip angle 30° (pulse width 3.0 ms); acquisition time, 1.36 s; repetition rate, 2.35 s; sweep width, ±6024 Hz. Spectral parameters for <sup>13</sup>C NMR: <sup>13</sup>C tip angle 40° (pulse width, 3.0 μs); acquisition time, 819.2 ms; repetition rate, 1.31 s; sweep width

$\pm 20000$  Hz. The pH values reported herein were determined with a pH-meter (Corning, Model 125) equipped with an Orion electrode. GC was performed by using a HP 5890 Series II gas chromatograph equipped with a FID detector, a Supelcowax<sup>®</sup> 10 capillary column (30 m, 0.32 mm I.D.) and a DB-1 capillary column (30 m, 0.25 mm I.D.). GC-MS analysis was done on a Hewlett-Packard 5890/MSD 5970 instrument in the EI mode with the same DB-1 capillary column. The following conditions were used for all gas chromatographic runs unless otherwise noted: oven temperature, 50°; initial value, 50°; rate, 10°/min; final temperature, 160°; final time, 5 min; injector temperature, 250°; detector temperature, 250°; flow, approximately 1–2 ml/min; sample volume, 1  $\mu$ l. The amounts of starting materials and products were calibrated directly by injecting known concentrations of authentic cyclohexene, cyclohexene oxide, cyclohexen-1-ol and cyclohexen-1-one to construct a calibration curve, hereafter referred to as calibrated GC.

#### 4.3. Cyclohexene oxidation procedure

The oxidation of cyclohexene was carried out under 1 atm oxygen in a constant temperature bath at  $38 \pm 0.1$  °C. The following standard procedure was used for all oxidation runs unless noted otherwise.

A 25 ml side-arm round-bottomed flask, equipped with a septum and a 10 mm magnetic stir bar was transferred into the drybox. Catalyst (50 mg;  $8.82 \times 10^{-3}$  mmol in case of **1**) was dissolved in the 25 ml round-bottomed flask using 6 ml of solvent. Then, freshly distilled cyclohexene (1 ml, 9.87 mmol) was added to the solution; in all runs a small amount of cyclohexene hydroperoxide (0.14 mmol) was also added to minimize the observed induction period [16] during the first 4–6 h reaction time. The flask was then sealed and brought immediately out of the drybox. The flask was then attached to the oxidation apparatus (see Fig. 1 elsewhere [16]), cooled to  $-196$  °C (77 K) with liquid nitrogen after which the whole system was freeze-pump-thaw degassed three times using the vacuum line that is part of the apparatus [16], and refilled with 1 atm of oxygen. The reaction vessel, now under 1 atm O<sub>2</sub>, was then placed in the constant temperature bath (Fischer Scientific), warmed up to  $38 \pm 0.1$  °C and vigorously stirred ( $\geq 800$  rpm) with the stir bar.

The reaction was then periodically sampled by syringe and analyzed by authentic-sample-calibrated GC. Time  $t = 0$  was defined after the oxygen had been added and the solution warmed up to  $38 \pm 0.1$  °C (a small error of 2–3 min is negligible compared to an average of 24 h, and in some cases up to 48 h, reaction time).

Cyclohexen-1-one, cyclohexen-1-ol and cyclohexene oxide were found to be the main, non-peroxidic products of the oxidation reaction; ca. 70 other products have been detected at higher conversion for this free-radical-chain autoxidation as described in detail elsewhere [16].

#### 4.4. Isolation of the active catalyst

The active catalyst was isolated from an oxidation run as described in Section 4.3, but scaled up by a factor of 10. In the drybox, 500 mg (0.088 mmol) of **1** was dissolved in a 250 ml round-bottomed flask using 60 ml of dichloromethane. Then 10 ml (98.7 mmol) of freshly distilled cyclohexene was added to the solution. After the addition of 25 mg (0.22 mmol) of 2-cyclohexen-1-yl hydroperoxide the flask was sealed and then immediately brought out of the drybox. The flask was then attached to the oxidation apparatus and the oxidation reaction was started as described in Section 4.3. After 50 h the reaction was stopped and the resulting suspension was allowed to cool to room temperature. During this time a brown-amber precipitate accumulated at the bottom of the reaction flask. This precipitate was collected by gravity filtration and washed three times with 2 ml of fresh CH<sub>2</sub>Cl<sub>2</sub>. The precipitate was then tested in fresh cyclohexene oxidation reaction according to the experimental procedure given in Section 4.3; it exhibits a low catalytic activity, essentially that of the background reaction (see Table 1, entries II and XIV), in part probably due to its low solubility in the CH<sub>2</sub>Cl<sub>2</sub>/cyclohexene reaction mixture.

The clear, yellow filtrate of the reaction solution (now minus the brown precipitate), was transferred into a 200 ml round-bottomed flask and the solvent and any remaining unreacted cyclohexene were removed by rotary evaporation using a water bath temperature of 55 °C. The remaining red-brown oily liquid (ca. 1–2 ml) was then triturated five times with 5 ml of *n*-hexane, followed by trituration

with diethylether (five times with 5 ml) to remove organic contaminants (such as remaining unreacted cyclohexene and higher boiling and polymeric cyclohexene oxidation products [16]). A yellow-orange solid resulted, which was collected and dried in vacuo at room temperature for 24 h. The yellow-orange product was then redissolved in approximately 2 ml of dichloromethane, and the resultant red-brown solution was filtered through a glass pipette containing a small amount of filter paper. The solvent was then removed and the yellow-orange solid was dried overnight under vacuum and at room temperature. The yellow-orange solid (i.e., “isolated catalyst”, 225.5 mg, ca. 45% of the weight of the starting material, **1**) is soluble in dichloromethane and acetonitrile; it was stored within the drybox for the duration of this study. The catalytic activity of the isolated material was tested as described in Section 4.5. The isolated catalyst material was characterized by elemental analysis, IR,  $^1\text{H}$ ,  $^{13}\text{C}$ ,  $^{31}\text{P}$  NMR, solution molecular weight measurement, and mass spectroscopy. Elemental analysis: % calc(found) for  $\text{C}_{96}\text{H}_{219}\text{IrN}_6\text{Na}_3\text{Nb}_3\text{O}_{65}\text{P}_2\text{W}_{15}$  {i.e., as  $[(n\text{-Bu}_4\text{N})_6\text{Na}_3(\text{HO})_3\text{Ir}^{3+}\cdot\text{P}_2\text{W}_{15}\text{Nb}_3\text{O}_{62}]_x$ }: C, 19.68(20.06); H, 3.77(3.77); Ir, 3.28(3.64); N, 1.43(1.30); Na, 1.18(1.37); Nb, 4.76(4.95); P, 1.06(1.08); W, 47.08(45.16). IR (KBr pellet,  $\text{cm}^{-1}$ ) polyoxometalate region 1080(vs), 1065(m), 940(s), 910(s), 895(s), 780(vs), 525(m).  $^{31}\text{P}$  NMR, in  $\text{CD}_3\text{CN}$ , 25 mg Kryptofix<sup>®</sup> added,  $\delta$  (# of P,  $\Delta\nu_{1/2}$ ) (Fig. 6a)  $-6.8$  (1 P,  $2.1 \pm 0.1$  Hz),  $-13.7$  (1 P,  $2.0 \pm 0.1$  Hz).  $^{183}\text{W}$  NMR, in  $\text{CD}_3\text{CN}$ , S/N after 10200 scans 28/1,  $\delta$  (# of W,  $\Delta\nu_{1/2}$ ) (Fig. 6b)  $-124$  (3 W,  $3 \pm 1$  Hz),  $-155$  (6 W,  $4 \pm 1$  Hz),  $-198$  (6 W,  $3 \pm 1$  Hz). Solution molecular weight determination: 10,900 MW (250 nm, 20,000 rpm), 7900 MW (250 nm, 30,000 rpm).

Attempts were made, using  $^1\text{H}$  NMR and  $^{13}\text{C}$  NMR, to determine the fate of the 1,5-COD ligand present in the precatalyst **1**. We attempted to compare the obtained spectra with results found by Klemperer and others [21] for the  $[(n\text{-Bu}_4\text{N})_2[(1,5\text{-COD})\text{Ir}\cdot\text{P}_3\text{O}_9]]$  analog, specifically for the following compounds:  $[(n\text{-Bu}_4\text{N})_2[(\text{C}_8\text{H}_{11}\text{OH})\text{Ir}\cdot\text{P}_3\text{O}_9]]$ ;  $^{13}\text{C}\{^1\text{H}\}$  NMR (75.5 MHz,  $\text{CD}_3\text{CN}$ ,  $20^\circ\text{C}$ , 0.07 M):  $\delta$  87.8, 74.7, 44.9, 44.8, 39.4, 37.9, 31.8, 27.2;  $^{31}\text{P}$  NMR (121.5 MHz,  $\text{CDCl}_3$ ,  $20^\circ\text{C}$ , 0.04 M):  $\delta$   $-1.1$ (dd),  $-3.3$ (dd),  $-8.4$ (dd);  $[(n\text{-Bu}_4\text{N})_2[(\text{C}_8\text{H}_{12}\text{OH})\text{Ir}\cdot\text{P}_3\text{O}_9]\cdot\text{C}_4\text{H}_8\text{O}]$ ;  $^{13}\text{C}\{^1\text{H}\}$  NMR (75.5 MHz,  $\text{CD}_3\text{CN}$ ,  $20^\circ\text{C}$ ,

0.26 M):  $\delta$  89.8, 80.3, 65.2, 34.7, 27.7, 26.1, 20.5,  $-3.9$ ;  $^{31}\text{P}$  NMR (121.5 MHz,  $\text{CDCl}_3$ ,  $20^\circ\text{C}$ , 0.02 M):  $\delta$   $-4.1$ (q),  $-4.6$ (q),  $-8.0$ (dd);  $[(n\text{-Bu}_4\text{N})_4\{[(1,5\text{-COD})(\text{O})\text{Ir}\cdot\text{P}_3\text{O}_9]_2\}]$ ;  $^{13}\text{C}\{^1\text{H}\}$  NMR (75.5 MHz,  $\text{CD}_3\text{CN}$ ,  $-20^\circ\text{C}$ ):  $\delta$  99.4, 93.1, 79.5, 78.9, 33.8, 33.1, 30.2, 28.3;  $^{31}\text{P}$  NMR (121.5 MHz,  $\text{CD}_2\text{Cl}_2$ ,  $-20^\circ\text{C}$ , 0.02 M):  $\delta$   $-12.4$ (q),  $-13.5$ (q),  $-21.6$ (dd). However, we were unable to obtain any conclusive evidence about the fate of the  $(1,5\text{-COD})\text{Ir}^+$  moiety. A broad signal (ca. 0.5 ppm) centered around 2.2 ppm was identified as residual  $\text{H}_2\text{O}$  and confirmed by adding  $\text{H}_2\text{O}$  to the original sample in a control experiment. No signals other than those associated with the  $n\text{-Bu}_4\text{N}^+$  cations were found by  $^1\text{H}$  and  $^{13}\text{C}$  NMR;  $^1\text{H}$  NMR ( $\text{CD}_3\text{CN}$ ):  $\delta$  1.04, 1.56, 1.72, 3.35;  $^{13}\text{C}$  NMR ( $\text{CD}_3\text{CN}$ ):  $\delta$  14.0, 19.8, 23.7, 58.1.

#### 4.5. Confirmation of the catalytic activity of the isolated catalyst

Using a sample of the isolated catalyst obtained in Section 4.4 above, a cyclohexene oxidation was carried out under 1 atm oxygen in a constant temperature bath at  $38 \pm 0.1^\circ\text{C}$ . Specifically, a 25 ml side-arm round-bottomed flask, equipped with a septum and a 10 mm magnetic stir bar was transferred into the drybox, and 50 mg of the isolated catalyst was dissolved in the 25 ml round-bottomed flask using 6 ml of dichloromethane. Then, freshly distilled cyclohexene (1 ml, 9.87 mmol) was added to the solution, the flask was sealed and then brought immediately out of the drybox. The flask was then attached to the oxidation apparatus, cooled to  $-196^\circ\text{C}$  (77 K) with liquid nitrogen and the whole system was degassed three times using its connection to the vacuum line and by refilling the system each time with 1 atm oxygen. Next, the reaction vessel, now under 1 atm  $\text{O}_2$ , was placed in the constant temperature bath, warmed up to  $38 \pm 0.1^\circ\text{C}$  and vigorously stirred with the stir bar ( $>800$  rpm). First, the catalytic activity of the isolated material was tested immediately after its isolation (described in Section 4.4). It proved to be essentially identical with those of the starting material **1** in two independent experiments (see Table 1, entry XIV, lines 1 and 2). A cyclohexene conversion of 23% (Table 1, entry XIV, line 1) was found after 24 h for the isolated catalyst (vs. 25% for the precatalyst, see Table 1, entry IV), along

Table 3  
Ultracentrifugation of molecular weight measurements

Experiment no.	Sample (calculated MW)	Wavelength employed	Molecular weight (observed, $\pm \sim 500$ )
I	$[n\text{-Bu}_4\text{N}]_9\text{P}_2\text{W}_{15}\text{Nb}_3\text{O}_{62}$ (6272)	250 nm	5500 <sup>a</sup> , 5700 <sup>b</sup>
II	Isolated catalyst; from reaction solution (after 310 turnovers)	250 nm	10900 <sup>a</sup> , 7900 <sup>b</sup>
III	$[n\text{-Bu}_4\text{N}]_5\text{Na}_3[(1,5\text{-COD})\text{Ir}\cdot\text{P}_2\text{W}_{15}\text{Nb}_3\text{O}_{62}]$ (5672)	320 nm	6100
IV	Reaction solution (after 310 turnovers)	320 nm	6100
V	Precipitate recovered from reaction solution (after 310 turnovers)	330 nm, 280 nm	10500, 10500

<sup>a</sup> Speed 20,000 rpm.

<sup>b</sup> Speed 30,000 rpm.

with 12% cyclohexen-1-one, 9% cyclohexen-1-ol, and 2% cyclohexene oxide, as the observed, non-peroxidic products. The isolated catalyst was again tested for its catalytic activity after 4 days using an identical procedure. It was found that the material had lost most of its activity (see Table 1, entry XIV, line 3).

#### 4.6. Attempts at growing single crystals of the isolated catalyst

Attempts to grow crystals of the isolated catalyst suitable for X-ray crystallography were made using vapor diffusion methods (acetonitrile, dichloromethane, and dichloroethane as solvents) at room temperature as well as at  $-20^\circ\text{C}$ . To date, none of these efforts have proven successful.

#### 4.7. TEM of the reaction solution and the precipitate

Transmission electron micrographs were taken at the University of Oregon on a Philips CM-12 with an  $70\ \mu\text{m}$  lens operated at 100 kV. Samples were prepared as before [12c,d] by spraying the solution onto copper grids covered with an amorphous-carbon thin film. Control experiments showed that the same TEM image was obtained whether the sample was sprayed in nitrogen or air. An control experiment showed that changing the voltage (40 kV vs. 100 kV) or the exposure time (seconds vs. minutes) did not change the TEM images; hence, the samples appear to be TEM-beam stable. In addition, all samples were examined at both low (100 kV) and high (430 kV) magnification from at least three randomly chosen areas as previously described in detail [12c,d].

#### 4.8. Solution molecular weight experiments

The results in entries I and II in Table 3 were obtained at Colorado State University in a Beckman XL-I ultracentrifuge at  $25^\circ\text{C}$  using a 60 Ti rotor. Absorbance data were collected at  $\lambda = 250\ \text{nm}$  using quartz windows and a two-channel charcoal-filled Epon centerpiece with a 12 mm pathlength. Prior to use, the centerpiece was “siliconized” by dipping it into a 5% solution of dimethyldichlorosilane (Fluka) in  $\text{CH}_2\text{Cl}_2$  (Fisher) for 2 min. For each experiment  $200\ \mu\text{l}$  of the sample solution was placed in one channel of the centerpiece and  $220\ \mu\text{l}$  of  $0.1\ \text{M}$   $[n\text{-Bu}_4\text{N}]\text{PF}_6$  in acetonitrile was placed in the other channel. At 2 h intervals (following an initial 12 h delay) 25 radial scans (using a  $0.003\ \text{cm}$  step size) were averaged. Equilibrium was assured by subtracting successive data sets.

Data analysis was performed in the XL-A/XL-I Data Analysis Software, Version 4.0 (Beckman Instruments) operating within Origin 4.1. The data were fit to an ideal, single-species model using the following equation:

$$C_r = C_m \exp \left[ \frac{M(1 - \bar{v}\rho)\omega^2(r^2 - r_m^2)}{2RT} \right]$$

where  $C_r$  is the concentration at some radial position,  $C_m$  the concentration at some reference position,  $M$  the weight-average molecular weight,  $\bar{v}$  the partial specific volume,  $\rho$  the solvent density,  $\omega$  the angular velocity,  $r$  the radial distance from the center of rotation,  $r_m$  the radial distance from the center of rotation to the reference position,  $R$  the gas constant, and  $T$  is the temperature in Kelvin. The solution density was taken to be  $0.78\ \text{g/ml}$  [6a]. The partial specific volume was approximated as  $0.389\ \text{ml/g}$ . This value for the par-

tial specific volume corresponds to the average value for similar compounds under similar conditions [6a], a case in which partial specific volume is not expected to vary significantly [6a,34].

The solution molecular weight  $[n\text{-Bu}_4\text{N}]_9\text{P}_2\text{W}_{15}\text{Nb}_3\text{O}_{62}$  was determined as a control experiment. All of the solution molecular weights have been given 5% error bars. Error bars of 5% are sufficient to assure that any time a compound's solution molecular weight was determined more than once, all of the results for that compound are the same within this  $\pm 5\%$  experimental error. This is true even if the extreme values of partial specific volume from reference [6a] are used instead of the average values.

Entries III–V of the ultracentrifuge sedimentation-equilibrium solution molecular weights in Table 3 were obtained at the University of Oregon on a Beckman Instruments Spinco Model E ultracentrifuge equipped with a scanning photoelectric system and an on-line IBM-compatible computer. Samples for MW determinations were prepared dissolving the sample in 0.1 M  $[n\text{-Bu}_4\text{N}]\text{PF}_6/\text{CH}_3\text{CN}$  electrolyte solution and the concentration of the sample adjusted so that the absorbance at the desired wavelength falls between 0.3 to 0.6 absorbance units. The sample was then injected into a doubly sectored cell, loaded into a rotor, and then spun at a speed of 20,000 rpm. After sedimentation-equilibrium was achieved (approximately 24 h), the concentration vs. distance data were collected and analyzed as described previously [6a,10a,12c]. The specific sample of the catalyst solution was the same as the one used for the TEM shown in Fig. 4a. In the case of the air-sensitive precatalyst, everything was done as indicated above, except that the precatalyst, **1**, was loaded into the cell in a drybox, details given in Section 4 in p. 1424 elsewhere [10a]. The results of the solution-equilibrium molecular weight measurements are summarized in Table 3.

#### 4.9. FAB mass spectroscopy

FAB-MS, in both positive ion and negative ion modes, was obtained at Oregon State University and following our earlier protocols [30]. The solid powders were dissolved directly in the FAB matrix, dithiothreitol/dithioerythritol (5:1), and then placed directly onto the stainless steel probe. Most analyses were carried out at mass resolutions of 1000, using

raw data (integrated multichannel averaging) or centroided data collection on a Kratos MS-50 mass spectrometer. Xenon gas was used to generate the primary ionizing beam from an Ion-Tech FAB gun operated at 7–8 keV. Further details on polyoxoanion FAB-MS are available elsewhere for the interested reader [30].

#### 4.10. Ion-exchange resin experiments for inner-sphere $M^{n+}$ to polyoxoanion bonding

The ion-exchange experiments were carried out in order to demonstrate the non-ion-exchangeability from the polyoxoanion of the  $\text{Ir}(\text{COD})^+$  moiety in **1** before, and of the oxidized  $\text{Ir}^{n+}$  after, the cyclohexene oxygenation. All manipulations were performed outside of the drybox. Macroreticular, strongly acidic ion-exchange resin (5 g; Amberlyst 15;  $\text{H}^+$  form; P-SO<sub>3</sub>H) was placed in a beaker together with ca. 20 ml of degassed water. The resin was swirled for ca. 2 min, followed by removal of the water using a disposable plastic pipette. This process was repeated until the aqueous phase was clear and colorless. The resin was then packed onto a 35.0 cm  $\times$  1.2 cm (length  $\times$  diameter) column. Then, 20 ml of degassed 40%  $n\text{-Bu}_4\text{N}^+\text{OH}^-/\text{H}_2\text{O}$  was diluted by ca. 1 part in 10 with distilled water and then passed dropwise through the column. When the eluant tested basic with pH paper (S/P<sup>®</sup> pH Indicator strips, Baxter Diagnostics), distilled water was passed through the column until the eluant tested neutral with the same pH paper. The resultant P-SO<sub>3</sub><sup>-</sup> $n\text{-Bu}_4\text{N}^+$  column was then washed with four 25 ml portions of acetonitrile (Aldrich). A solution of ca. 40 mg of **1** in 1 ml of CH<sub>3</sub>CN was then loaded onto the column. The brown solution passed through the column dropwise, with no apparent retention. The brown eluant was collected, and the solvent removed by rotary evaporation under reduced pressure. The IR spectrum (KBr pellet) of 2 mg of the colored residue was recorded from 400 to 1200  $\text{cm}^{-1}$  showing the characteristic IR absorptions of the Dawson-type  $\text{P}_2\text{W}_{15}\text{Nb}_3\text{O}_{62}^{9-}$  polyoxoanion.

An anion-exchange column of identical size was packed with strongly basic resin (Amberlyst A-27;  $\text{Cl}^-$  form; P-NR<sub>3</sub><sup>+</sup> $\text{Cl}^-$ ) and was then washed with acetonitrile. A sample of **1** was loaded onto the column as described above for the cation-exchange resin. All of the brown sample was retained on the resin in the upper half of the column.

The experimental procedure described above for **1** was then repeated exactly, only now using 40 mg of the isolated catalyst from Section 4.4. Non-ion-exchangeability, analogous to that described above for authentic precatalyst **1**, was found for the isolated catalyst material.

These results demonstrate that neither the Ir(1,5-COD)<sup>n+</sup> in the precatalyst, nor the oxidized iridium component of the isolated catalyst, are cleaved from the polyoxoanion support under the oxidation catalysis condition applied in this study, the latter not even after 48 h (ca. 310 total turnovers) of cyclohexene autoxidation.

#### 4.11. Experiments demonstrating the cleavage of Ir-polyoxometalate bonding in the precatalyst **1**, and also in the isolated catalyst

A solution of **1** was prepared by dissolving 250 mg (0.09 mmol) in 2 ml CD<sub>3</sub>CN; 245 mg (0.89 mmol; 20 equiv.) of *n*-Bu<sub>4</sub>N<sup>+</sup>Cl<sup>-</sup> was then added. No visible change in solution color could be observed. The <sup>31</sup>P NMR spectrum (acquired in the presence of 3 equiv. Kryptofix<sup>®</sup> 2.2.2 to remove Na<sup>+</sup> ion-pairing effects [10b]) showed two lines: <sup>31</sup>P NMR (22 °C, 22 mM, CD<sub>3</sub>CN) δ: -6.3; -13.6 (±0.4), chemical shifts characteristic of the free, parent P<sub>2</sub>W<sub>15</sub>Nb<sub>3</sub>O<sub>62</sub><sup>9-</sup> [10]. The downfield shift of the phosphorus resonance closer to the “Nb<sub>3</sub>O<sub>9</sub><sup>3-</sup>” cap, δ -6.3 ppm, compared to that in the precatalyst, δ -7.2 ppm, is further evidence for cleavage of [1,5-COD]Ir<sup>+</sup>, most likely as [(1,5-COD)IrCl]<sub>2</sub>, from the heteropolyoxoanion support with concomitant reformation of the starting P<sub>2</sub>W<sub>15</sub>Nb<sub>3</sub>O<sub>62</sub><sup>9-</sup>.

In the drybox, 150 mg of **1**, and 150 mg of the isolated catalyst were placed in two, separate 19 mm × 50 mm disposable glass vials containing 10 mm Teflon-coated magnetic stir bars. Then, approximately 1 ml of a mixture of CH<sub>3</sub>CN/D<sub>2</sub>O (20/80) was added to each vial, and the mixtures were each stirred for about 30 min. The resulting two, yellow-brown solutions were then placed in two separate, airtight NMR tubes (J. Young airtight valve; Wilmad). The <sup>31</sup>P NMR spectra show the familiar two-line spectrum [10] (-6.3 ± 0.4 ppm; -13.5 ± 0.4 ppm) characteristic of the free, parent [n-Bu<sub>4</sub>N]<sub>9</sub>P<sub>2</sub>W<sub>15</sub>Nb<sub>3</sub>O<sub>62</sub>, indicating that the Ir-polyoxometalate bonding present in the isolated catalyst had been cleaved.

The following procedure was carried out outside of the drybox under argon. First, 250 mg of **1**, and then 250 mg of the isolated catalyst, were placed in two separate 25 mm × 55 mm glass vials containing 10 mm Teflon-coated magnetic stir bars. Next, approximately 5 ml of deionized H<sub>2</sub>O was added to each vial, and the pH was adjusted to 1.5 (pH-meter) using 1:1 diluted hydrochloric acid; the resultant, two separate mixtures were each stirred for about 30 min. The resulting precipitates were each collected on separate, 2 ml medium-glass frits and dried over night under vacuum at room temperature. The two precipitates (approximately 150 mg each) were then dissolved in separate 1 ml portions of CD<sub>3</sub>CN and transferred into separate NMR tubes (5 mm o.d.). The individual <sup>31</sup>P NMR spectra for the two materials showed the previously reported spectrum (-12.1 ± 0.3 ppm; -11.9 ± 0.3 ppm; -9.7 ± 0.3 ppm; -9.5 ± 0.3 ppm) characteristic of the protonated, supported-metal-free [n-Bu<sub>4</sub>N]<sub>5</sub>H<sub>4</sub>P<sub>2</sub>W<sub>15</sub>Nb<sub>3</sub>O<sub>62</sub> [7a].

The results of the above experiments show: (i) that the cleavage of the iridium-polyoxometalate bonding can directly be monitored by <sup>31</sup>P NMR spectroscopy; (ii) that deliberate cleavage of the iridium-polyoxometalate bond can be accomplished by the addition of a large excess of Cl<sup>-</sup> in the case of the precatalyst, or by the addition of H<sub>2</sub>O or H<sup>+</sup> in the cases of both the precatalyst and the isolated catalyst; (iii) that in all three cases the cleavage of the organometallic iridium moiety leads to the formation of the parent, polyoxometalate (or its protonated form); and (iv) most importantly, that iridium-polyoxometalate bonding is present in the isolated catalyst and before treatment with Cl<sup>-</sup>.

#### 4.12. The oxidation of [(1,5-COD)Ir(CH<sub>3</sub>CN)<sub>2</sub>]BF<sub>4</sub>

In the drybox, 500 mg (1.06 mmol) [(1,5-COD)Ir-(CH<sub>3</sub>CN)<sub>2</sub>]BF<sub>4</sub>, prepared from [(1,5-COD)IrCl]<sub>2</sub> and AgBF<sub>4</sub> as described elsewhere [10a], was dissolved in 40 ml dichloromethane using a 100 ml round-bottomed flask containing a 10 mm Teflon-coated magnetic stir bar. The flask was then sealed using a rubber septum and transferred outside of the drybox. The reaction flask was then cooled to -78 °C in a dry ice-ethanol bath and oxygen gas was bubbled through the solution at this temperature for 2 h. The solution was then warmed up to -20 °C and stirred

for another 4 h at  $-20^{\circ}\text{C}$ . After approximately the first 2 h at  $-20^{\circ}\text{C}$ , the color of the bright-yellow solution turns slowly into a deeper yellow and then, later, to yellow-brown while also becoming cloudy, producing a brown precipitate. The mixture was finally allowed to warm up to room temperature and stirred under 1 atm oxygen overnight. The solvent was then removed under vacuum at room temperature. Next, 25 ml dichloromethane was then added to the yellow-brown residue, and the mixture was stirred for 1 h at room temperature. The resulting deep-yellow solution was separated from a remaining brown precipitate by filtration; the precipitate was then extracted five times with 2 ml of fresh dichloromethane, and the fractions were combined with the first, deep-yellow filtrate. The remaining brown precipitate (198 mg, 40%) was finally washed twice with 2 ml of diethyl ether and dried under vacuum overnight at room temperature. The combined filtrates were dried by removing the solvent in vacuum at room temperature, the resulting yellow solid (137 mg, 27%) was also washed twice with 2 ml diethyl ether and dried under vacuum overnight.

The yellow solid obtained from the reaction solution is soluble in dichloromethane and acetonitrile, whereas the brown precipitate is insoluble in dichloromethane. Both materials were independently tested for their catalytic activity in cyclohexene autoxidation; only low activity ( $<8\%$  conversion), essentially none above background, was observed for both materials (Table 1, entries IX and X in comparison to entry II) and in the absence of any added  $[n\text{-Bu}_4\text{N}]_9\text{P}_2\text{W}_{15}\text{Nb}_3\text{O}_{62}$ . Approximate molecular formulas for each material were established by elemental analysis (all elements, except boron). Solid A (yellow, from reaction solution): found (%), C, 33.11; H, 4.63; N, 4.43; F, 13.6; Ir, 34.70; O, 2.76. The results found for solid A, recovered from the reaction solution, give the empirical formula  $\text{C}_{11}\text{H}_{1.67}\text{N}_{0.12}\text{O}_{0.07}\text{Ir}_{0.07}\text{B}_{0.06}\text{F}_{0.26}$ , that is,  $[\text{C}_{15}\text{H}_{25}\text{N}_{1.72}\text{O}_1\text{Ir}_1\text{B}_1\text{F}_4]$ , a result which is perhaps within experimental error (for this non-crystalline sample) of  $[(\text{C}_8\text{H}_{12})(\text{O})\text{Ir}(\text{CH}_3\text{CN})_2\text{BF}_4]$ . For solid B (the brown precipitate): found (%), C, 24.57; H, 3.44; N, 3.31; F, 13.4; Ir, 40.70; O, 5.80; these results lead to a formulation of  $\text{C}_{11}\text{H}_{1.67}\text{N}_{0.12}\text{O}_{0.18}\text{Ir}_{0.10}\text{B}_{0.09}\text{F}_{0.34}$  or  $\text{C}_{10}\text{H}_{16.7}\text{N}_{1.2}\text{O}_{1.8}\text{Ir}_{1.0}\text{B}_{0.9}\text{F}_{3.4}$ , something perhaps approaching  $[(\text{C}_8\text{H}_{12})(\text{O})_2\text{IrBF}_4]$ , although this

was not pursued further since this brown precipitate proved uninteresting catalytically, even in the presence of added polyoxoanion (vide infra). Infrared measurements on both materials confirm the presence of  $\text{BF}_4^-$  (KBr pellet,  $\text{cm}^{-1}$ ,  $\nu = 1040\text{ cm}^{-1}$ ).

#### 4.13. Independent synthesis of the active catalyst

In the drybox,  $[n\text{-Bu}_4\text{N}]_9\text{P}_2\text{W}_{15}\text{Nb}_3\text{O}_{62}$  (1 g, 0.09 mmol) was dissolved in 10 ml dichloromethane in a 25 ml round-bottomed flask that contained a 10 mm magnetic stirrer bar. A solution of 55 mg of the oxidation product of  $[(1,5\text{-COD})\text{Ir}(\text{MeCN})_2]\text{BF}_4$ , obtained from the reaction solution (see Section 4.12), was placed in 5 ml of dichloromethane, and this homogeneous solution was then added to the polyoxometalate solution. The resulting clear, yellow-brown solution was stirred for 1 h at room temperature. The reaction mixture was then evacuated to dryness and dried under vacuum for 4 h. Reprecipitation of the crude product was accomplished by first dissolving it in 0.5 ml acetonitrile, and then, after filtration, adding it (over ca. 1–2 min) under stirring to 100 ml of ethylacetate. The final product (210 mg, 21% of the weight of the  $[n\text{-Bu}_4\text{N}]_9\text{P}_2\text{W}_{15}\text{Nb}_3\text{O}_{62}$  starting material) was then collected by gravity filtration (Whatman #2 filter paper), washed twice with ca. 1 ml of diethyl ether and dried under vacuum overnight at room temperature. The product was characterized by IR spectroscopy,  $^{31}\text{P}$  and  $^{183}\text{W}$  NMR spectroscopy. IR (KBr pellet,  $\text{cm}^{-1}$ ) polyoxometalate region 1082(vs), 1064(m), 1012 (w), 946(s), 893(s), 780(vs), 525(m).  $^{31}\text{P}$  NMR, in  $\text{CD}_3\text{CN}$ , 25 mg Kryptofix<sup>®</sup> added,  $\delta$  (# of P,  $\Delta\nu_{1/2}$ ),  $-7.2$  (broad),  $-13.3$  (1 P,  $2.0 \pm 0.2$  Hz).  $^{183}\text{W}$  NMR ( $\text{CD}_3\text{CN}$ , ca. 55 mM),  $\delta$  (# of W,  $\Delta\nu_{1/2}$ ),  $-128$  (3 W,  $4 \pm 1$  Hz),  $-144$  (6 W,  $4 \pm 1$  Hz),  $-196$  (6 W,  $4 \pm 1$  Hz). The catalytic activity was tested immediately after the isolation of the product. Significantly, the initial catalytic activity of this “synthesized catalyst” proved to be essentially identical with  $[n\text{-Bu}_4\text{N}]_5\text{Na}_3[(1,5\text{-COD})\text{Ir}\cdot\text{P}_2\text{W}_{15}\text{Nb}_3\text{O}_{62}]$ , **1** (cf. Table 1, entries XVI, XIV and IV).

The synthesis procedure described above was repeated using the brown precipitate, recovered from the oxidation of  $[(1,5\text{-COD})\text{Ir}(\text{MeCN})_2]\text{BF}_4$ . Due to its insolubility in dichloromethane the procedure was carried out using acetonitrile as solvent, but all other steps were identical to the above procedure. The resulting

brown solid was found to be inactive in a standard (ROOH initiated) cyclohexene oxidation (<5% cyclohexene conversion after 48 h).

#### 4.14. The stoichiometric oxidation of the catalyst precursor

$[n\text{-Bu}_4\text{N}]_5\text{Na}_3[(1,5\text{-COD})\text{Ir}\cdot\text{P}_2\text{W}_{15}\text{Nb}_3\text{O}_{62}]$ , **1**

The oxidation product of **1** was prepared by reaction of  $[n\text{-Bu}_4\text{N}]_5\text{Na}_3[(1,5\text{-COD})\text{Ir}\cdot\text{P}_2\text{W}_{15}\text{Nb}_3\text{O}_{62}]$  with dioxygen in dichloromethane at room temperature, but in the absence of cyclohexene. In the drybox, 1.2 g (0.2116 mmol)  $[n\text{-Bu}_4\text{N}]_5\text{Na}_3[(1,5\text{-COD})\text{Ir}\cdot\text{P}_2\text{W}_{15}\text{Nb}_3\text{O}_{62}]$  was placed in a 100 ml side-arm round-bottomed flask, containing a stir bar. The round-bottomed flask was sealed and brought out of the drybox. A water cooled, reflux condenser was then attached and 45 ml dichloromethane was added. After bubbling oxygen through the solution for 1 h the reaction mixture was stirred for 10 h at room temperature. During the 10 h reaction time the reaction mixture becomes slightly cloudy, but there is little other visible change of the yellow-brown solution during the 10 h. Significantly, there is no formation of a precipitate under these cyclohexene-free conditions (i.e., and as is seen with added cyclohexene and, thus, under autoxidation conditions). The crude, yellow-brown material was then isolated by removing the solvent in vacuum at room temperature; it is soluble in dichloromethane, acetonitrile, methanol, dimethyl formamide and dimethyl sulfoxide. *Note: After storing the product under air for more than 2 weeks some white precipitate did form when the product was redissolved in dichloromethane.* The crude material was then dissolved in 200 ml of a 1:1 mixture of ethylacetate/acetonitrile and 25 g silica gel (silica gel 60 PF 254, Merck) was then added. The slurry was stirred for 2 h at room temperature, filtered through a glass frit, and the silica gel was rinsed with an additional 50 ml of 1:1 ethylacetate/acetonitrile; the silica gel remained with a light-brown color. The resulting yellow filtrates were combined, then evaporated to dryness at 40 °C using a rotary evaporator, followed by drying under vacuum overnight at room temperature. The yellow product was stored within the drybox for the duration of this study. Yield: 0.90–0.96 g; 75–80% of the crude material. This isolated oxidation product from the precatalyst **1** has been characterized by

IR spectroscopy, as well as by  $^{31}\text{P}$ , and  $^{183}\text{W}$  NMR spectroscopy. IR (KBr pellet,  $\text{cm}^{-1}$ ) polyoxometalate region 1084(vs), 1060(m), 1012 (w), 942(s), 912(s), 895(s), 788(vs), 524(m).  $^{31}\text{P}$  NMR, in  $\text{CD}_3\text{CN}$ , 25 mg Kryptofix<sup>®</sup> added,  $\delta$  (# of P,  $\Delta\nu_{1/2}$ ),  $-6.9$  (several lines of lower intensity),  $-13.6$ .  $^{183}\text{W}$  NMR, in  $\text{CD}_3\text{CN}$ ,  $\delta$  (# of W,  $\Delta\nu_{1/2}$ ),  $-126$  (3 W,  $3 \pm 1$  Hz),  $-149$  (6 W,  $4 \pm 1$  Hz),  $-191$  (6 W,  $4 \pm 1$  Hz). Significantly, the oxidized **1** proved to be ineffective in the cyclohexene autoxidation, see Table 1, entry XV.

#### 4.15. Oxygen uptake experiments

The stoichiometric reaction of  $[n\text{-Bu}_4\text{N}]_5\text{Na}_3[(1,5\text{-COD})\text{Ir}\cdot\text{P}_2\text{W}_{15}\text{Nb}_3\text{O}_{62}]$ , **1**,  $[n\text{-Bu}_4\text{N}]_2[(1,5\text{-COD})\text{Ir}\cdot\text{P}_3\text{O}_9]$ , and  $[(1,5\text{-COD})\text{IrCl}]_2$  with molecular oxygen in 1,2-dichloroethane were investigated using the a gas-uptake line connected to a calibration flask and a mercury manometer; calibration was accomplished as before [6k].

In the drybox, ca.  $3.0 \times 10^{-4}$  mol of one of the above three compounds was placed in a 50 ml round-bottomed flask equipped with a 10 mm Teflon-coated stir bar and dissolved by adding 10 ml of 1,2-dichloroethane. The flask was then sealed, brought out of the drybox and connected to the gas-uptake line. The reaction flask was then placed in an ethanol/dry ice bath (195 K;  $-78$  °C) for 30 min and the uptake line with calibration flask and reaction flask was then evacuated. The system was then refilled with 1 atm dioxygen, the connection to the calibration flask was then closed off, and the uptake-apparatus was again evacuated. The connection to the vacuum pump was then closed, and the oxygen in the calibration flask was released into the system. The ethanol/dry ice bath was then replaced with an ice/H<sub>2</sub>O bath, and the reaction mixture was stirred for 5 min to equilibrate at the reaction temperature of 273 K. The pressure after 5 min was defined as  $p$  at  $t = 0$ , and pressure readings were recorded thereafter every 30 min until no further change in pressure was observed (6–8 h). The pressure readings were corrected with a vapor–pressure calibration curve obtained for 1,2-dichloroethane under identical conditions (10 ml, 273 K). The results of the oxygen uptake experiments are summarized in Table 2.



#### 4.16. The catalytic activity of related compounds in cyclohexene autoxidation

Due to the apparent similarity, and thus potential relevance, of the  $\text{P}_3\text{O}_9^{3-}/(1,5\text{-COD})\text{Ir}^+$  system to our own study, several catalytic tests using  $\text{P}_3\text{O}_9^{3-}$  based catalyst materials were performed:

- (i) 10 mg ( $9.78 \times 10^{-3}$  mmol)  $[\text{n-Bu}_4\text{N}]_2[(1,5\text{-COD})\text{Ir}\cdot\text{P}_3\text{O}_9]$  [21a] was used as precatalyst in cyclohexene oxidation as described in Section 4.3. A catalytic activity of approximately 80% that of the activity of the polyoxoanion-supported iridium complex **1** was observed over ca. 300 turnovers, see Table 1, entry XI).
- (ii) 10 mg ( $9.63 \times 10^{-3}$  mmol) of its oxidized form,  $[\text{n-Bu}_4\text{N}]_2[(\text{C}_8\text{H}_{11}\text{OH})\text{Ir}\cdot\text{P}_3\text{O}_9]$  [21a] was used as precatalyst in a separate experiment for the catalytic cyclohexene oxidation. The material was found to be catalytically only slightly more active than an average background of  $\sim 9\%$ , see Table 1, entries XII and II.
- (iii) Based on the results of the approach to independently synthesize the active,  $\text{P}_2\text{W}_{15}\text{Nb}_3\text{O}_{62}^{9-}$  based catalyst, vide supra, both solids, obtained from the stoichiometric oxidation of  $[(1,5\text{-COD})\text{Ir}(\text{CH}_3\text{CN})_2]\text{BF}_4$ , were also used together with  $\text{P}_3\text{O}_9^{3-}$  in catalytic test experiments. Separately, 500 mg (0.49 mmol)  $[\text{n-Bu}_4\text{N}]_3\text{P}_3\text{O}_9\cdot 2.5\text{H}_2\text{O}$  [21a] was dissolved in 5 ml acetonitrile at room temperature using two 10 ml glass vials with magnetic stir bars (0.5 cm). Then, 25 mg of each solid was added separately to the  $[\text{n-Bu}_4\text{N}]_3\text{P}_3\text{O}_9$  solutions, and the resulting yellow-brown solutions were stirred for 30 min at room temperature. The solvents were then removed in vacuum at room temperature, the resulting solids were washed twice with 10 ml diethylether and dried overnight in vacuum. Ten milligram of each material was used in catalytic cyclohexene oxidation experiments. Only the material, obtained from  $[\text{n-Bu}_4\text{N}]_3\text{P}_3\text{O}_9$  plus the solid isolated from the reaction solution of the  $[(1,5\text{-COD})\text{Ir}(\text{CH}_3\text{CN})_2]\text{BF}_4$  oxidation (Section 4.12) was found to be now catalytically active in cyclohexene oxidation (18% conversion; see Table 1, entry XVII).

To measure the activity of other related compounds (e.g.  $[(1,5\text{-COD})\text{IrCl}]_2$ ,  $[\text{Ir}_2\text{O}(\text{OH})_2(1,5\text{-COD})_2\text{Cl}_2]$ ,  $[(1,5\text{-COD})\text{Ir}(\text{CH}_3\text{CN})_2]\text{BF}_4$ ) the same catalytic procedure was used as described above for the oxidation of cyclohexene (Section 4.3). The amount of catalyst used was adjusted to give the same concentration [1.26 mM] and the same [catalyst]/[cyclohexene] ratio, all as detailed in Section 4.3. The results of this survey are summarized in entries V–VIII of Table 1; in no case was significant activity above background detected.

#### Acknowledgements

We thank Dr. Brian Arbogast, Department of Agricultural Chemistry, Oregon State University, Corvallis, OR, for making available to us their Kratos MS-50 mass spectrometer and carrying out the FAB-MS measurements. Jason Widegren at Colorado State University is thanked for performing the ultracentrifugation MW measurement on the isolated catalyst. TEM measurements were made with the expert assistance of Dr. Eric Schabtach at the University of Oregon. Financial support was provided by the National Science Foundation, initially via grant CHE-9531110, and more recently via grant CHE-0078436.

#### References

- [1] (a) M.T. Pope, *Heteropoly and Isopoly Oxometalates*, Springer, New York, 1983;  
(b) V.W. Day, W.G. Klemperer, *Science* 228 (1985) 533;  
(c) M.T. Pope, A. Müller, *Angew. Chem. Int. Ed. Engl.* 30 (1991) 34.
- [2] Polyoxometalates: from platonic solids to anti-retroviral activity, in: A. Müller, M.T. Pope (Eds.), *Proceedings of the July 15–17, 1992 Meeting at the Center for Interdisciplinary Research in Bielefeld, Germany*, Kluwer Academic Publishers, Dordrecht, 1992.
- [3] Polyoxometalates, C.L. Hill (Ed.), *Chem. Rev.* 98 (1998) 1–390 (14 invited reviews).
- [4] L.C.W. Baker, in: S. Kirschner (Ed.), *Advances in the Chemistry of Coordination Compounds*, Macmillan, New York, 1961, p. 604.
- [5] J. Schwartz, *Acc. Chem. Res.* 18 (1985) 302.
- [6] (a) R.G. Finke, M.W. Droegge, *J. Am. Chem. Soc.* 106 (1984) 7274;  
(b) R.G. Finke, B. Rapko, P.J. Domaille, *Organometallics* 5 (1986) 175;  
(c) M.W. Droegge, Dissertation, University of Oregon, 1984;

- (d) B. Rapko, Dissertation, University of Oregon, 1986;  
(e) D.J. Edlund, R.J. Saxton, D.K. Lyon, R.G. Finke, *Organometallics* 7 (1988) 1692;  
(f) R.G. Finke, C.A. Green, B. Rapko, *Inorg. Syn.* 27 (1990) 128;  
(g) Y. Lin, K. Nomiya, R.G. Finke, *Inorg. Chem.* 32 (1993) 6040;  
(h) K. Nomiya, C. Nozaki, M. Kaneko, R.G. Finke, M. Pohl, *J. Organomet. Chem.* 505 (1995) 23;  
(i) R.G. Finke, K. Nomiya, C.A. Green, M.W. Droegge, *Inorg. Syn.* 29 (1992) 239;  
(j) M. Pohl, Y. Lin, T.J.R. Weakley, K. Nomiya, M. Kaneko, H. Weiner, R.G. Finke, *Inorg. Chem.* 34 (1995) 767;  
(k) T. Nagata, M. Pohl, H. Weiner, R.G. Finke, *Inorg. Chem.* 36 (1997) 1366.
- [7] (a) H. Weiner, J.D. Aiken III, R.G. Finke, *Inorg. Chem.* 35 (1996) 7905;  
(b) R.G. Finke, D.K. Lyon, K. Nomiya, T.J.R. Weakley, *Acta Crystallogr. C* 46 (1990) 1592;  
(c) K. Nomiya, M. Kaneko, N. Kasuga, R.G. Finke, M. Pohl, *Inorg. Chem.* 33 (1994) 1469;  
(d) B.J. Hornstein, R.G. Finke, *Inorg. Chem.* 41 (2002) 2720.
- [8] (a) D.E. Katsoulis, M.T. Pope, *J. Chem. Soc., Chem. Commun.* (1986) 1186;  
(b) K. Pieprgrass, M.T. Pope, *J. Am. Chem. Soc.* 111 (1989) 753.
- [9] (a) C.J. Besecker, W.G. Klemperer, *J. Am. Chem. Soc.* 102 (1980) 7598;  
(b) C.J. Besecker, V.W. Day, W.G. Klemperer, *Organometallics* 4 (1985) 564;  
(c) V.W. Day, M.F. Fredrich, M.R. Thompson, W.G. Klemperer, R.-S. Liu, W. Shum, *J. Am. Chem. Soc.* 103 (1981) 3597;  
(d) C.J. Besecker, V.W. Day, W.G. Klemperer, M.R. Thompson, *J. Am. Chem. Soc.* 106 (1984) 4125;  
(e) C.J. Besecker, V.W. Day, W.G. Klemperer, M.R. Thompson, *Inorg. Chem.* 24 (1985) 44;  
(f) C.J. Besecker, W.G. Klemperer, V.W. Day, *J. Am. Chem. Soc.* 104 (1982) 6158;  
(g) W.G. Klemperer, A. Yagasaki, *Chem. Lett.* (1989) 2041;  
(h) W.G. Klemperer, D.J. Main, *Inorg. Chem.* 29 (1990) 2355;  
(i) V.W. Day, W.G. Klemperer, D.J. Main, *Inorg. Chem.* 29 (1990) 2345;  
(j) V.W. Day, W.G. Klemperer, A. Yagasaki, *Chem. Lett.* (1990) 1267;  
(k) V.W. Day, W.G. Klemperer, *Polyoxometalates*, in: M.T. Pope, A. Müller (Eds.), Kluwer Academic Publishers, Dordrecht, 1994, pp. 87–104. Republished in: V.W. Day, W.G. Klemperer, *Mol. Eng.* 3 (1993) 61–78.
- [10] (a) M. Pohl, D.K. Lyon, N. Mizuno, K. Nomiya, R.G. Finke, *Inorg. Chem.* 34 (1995) 1413;  
(b) K. Nomiya, M. Pohl, N. Mizuno, D.K. Lyon, R.G. Finke, *Inorg. Syn.* 31 (1997) 186;  
(c) R.G. Finke, D.K. Lyon, K. Nomiya, S. Sur, N. Mizuno, *Inorg. Chem.* 29 (1990) 1784;  
(d) D.K. Lyon, Dissertation, University of Oregon, 1990.
- [11] M. Pohl, R.G. Finke, *Organometallics* 12 (1993) 1453.
- [12] (a) D.K. Lyon, R.G. Finke, *Inorg. Chem.* 29 (1990) 1787;  
(b) D.J. Edlund, R.G. Finke, J.R. Saxton, US Patent 5 116 796 (1992);  
(c) Y. Lin, R.G. Finke, *J. Am. Chem. Soc.* 116 (1994) 8335;  
(d) Y. Lin, R.G. Finke, *Inorg. Chem.* 33 (1994) 4891.
- [13] (a) N. Mizuno, D.K. Lyon, R.G. Finke, *J. Catal.* 128 (1991) 84;  
(b) N. Mizuno, D.K. Lyon, R.G. Finke, US Patent 5 250 739 (1993).
- [14] H. Weiner, Y. Hayashi, R.G. Finke, *Inorg. Chem.* 38 (1999) 2579.
- [15] (a) C.L. Hill, C.M. Prosser-McCartha, *Coord. Chem. Rev.* 143 (1995) 407;  
(b) C.L. Hill, *J. Mol. Catal.* 114 (1–3) (1996) 1–365;  
(c) N. Mizuno, M. Misono, *Mol. Catal.* 86 (1994) 319;  
(d) T. Okuhara, N. Mizuno, M. Misono, *Adv. Catal.* 41 (1996) 113;  
(e) I.V. Kozhevnikov, *Catal. Rev. Sci. Eng.* 37 (1995) 311;  
(f) R. Neumann, *Prog. Inorg. Chem.* 47 (1998) 317;  
(g) C.L. Hill (Guest Ed.), *Chem. Rev.* 98 (1) (1998) 1–389.
- [16] H. Weiner, A. Trovarelli, R.G. Finke, *J. Mol. Catal.* 191 (2003) 217–252.
- [17] F. Haber, *J. Weiss, Naturwissenschaften* 20 (1931) 948.
- [18] (a) K. Urabe, Y. Tanaka, Y. Izumi, *Chem. Lett.* (1985) 1595;  
(b) T.M. Che, US Patent 4 590 298 (20 May 1986), to Celanese Corp.;
- (c) A.R. Siedle, C.G. Markell, P.A. Lyon, K.O. Hodgson, A.L. Roe, *Inorg. Chem.* 26 (1987) 219;  
(d) A.R. Siedle, R.A. Newmark, W.B. Gleason, R.P. Skarjune, K.O. Hodgson, A.L. Roe, V.W. Day, *Solid State Ionics* 26 (1988) 109.
- [19] (a) K. Takao, Y. Fujiwara, T. Imanaka, S. Teranishi, *Bull. Chem. Soc. Jpn.* 43 (1970) 1153;  
(b) A. Fusi, R. Ugo, A. Pasini, S. Cenini, *J. Organometal. Chem.* 26 (1971) 417;  
(c) B.R. Sutherland, M. Cowie, *Organometallics* 4 (1985) 1637;  
(d) D. Milstein, J.C. Calabrese, I.D. Williams, *J. Am. Chem. Soc.* 108 (1986) 6387;  
(e) H.-H. Wang, L.H. Pignolet, P.E. Reedy Jr., M.M. Olmstead, A.L. Balch, *Inorg. Chem.* 26 (1987) 377;  
(f) W.D. McGhee, T. Foo, F.J. Hollander, R.G. Bergmann, *J. Am. Chem. Soc.* 110 (1988) 8543;  
(g) P. Barbaro, C. Bianchini, C. Mealli, A. Meli, *J. Am. Chem. Soc.* 113 (1991) 3181;  
(h) J. Xiao, B.D. Santarsiero, B.A. Vaartstra, M. Cowie, *J. Am. Chem. Soc.* 115 (1993) 3212;  
(i) J. Sundermeyer, *Angew. Chem. Int. Ed. Engl.* 32 (1993) 1144.
- [20] (a) R. Bonnaire, P. Fourgeroux, *CR Acad. Sci. Paris, Ser. C* 280 (1975) 767;  
(b) F.A. Cotton, P. Lahuerta, M. Sanau, W. Schwotzer, *Inorg. Chim. Acta* 120 (1986) 153.
- [21] (a) V.W. Day, W.G. Klemperer, S.P. Lockledge, D.J. Main, *J. Am. Chem. Soc.* 112 (1990) 2031;  
(b) V.W. Day, T.A. Ebersbacher, W.G. Klemperer, B. Zhong, *J. Am. Chem. Soc.* 116 (1994) 3119;

- (c) D.J. Main, Dissertation, University of Illinois, May 1987.
- [22] (a) A. Nutton, P.M. Bailey, P.M. Maitlis, *J. Organomet. Chem.* 213 (1981) 313;  
(b) P.M. Maitlis, *Acc. Chem. Res.* 11 (1978) 301;  
(c) J.W. Kang, P.M. Maitlis, *J. Organomet. Chem.* 30 (1971) 127;  
(d) A. Nutton, P.M. Bailey, P.M. Maitlis, *J. Chem. Soc., Dalton Trans.* (9) (1981) 1997;  
(e) K. Isobe, P.M. Bailey, P.M. Maitlis, *J. Chem. Soc., Dalton Trans.* (9) (1981) 2003;  
(f) F.A. Cotton, P. Lahuerta, M. Sanau, W. Schwotzer, *J. Chem. Soc.* 107 (1985) 8284;  
(g) D.J. Gulliver, W. Levason, *Coord. Chem. Rev.* 46 (1982) 1;  
(h) S. Uemura, A. Spencer, G. Wilkinson, *J. Chem. Soc., Dalton Trans.* (23) (1973) 2565;  
(i) K. Hirai, A. Nutton, P. Maitlis, *J. Mol. Catal.* 10 (1981) 203.
- [23] (a) H.J. Lawson, J.D. Atwood, *J. Am. Chem. Soc.* 110 (1988) 3680;  
(b) C. Bianchini, A. Meli, M. Peruzzini, F. Vizza, *J. Am. Chem. Soc.* 112 (1990) 6726.
- [24] (a) J.A. Howard, Homogeneous liquid phase autoxidations, in: J.K. Kochi (Ed.), *Free Radicals*, Vol. II, Wiley, New York, 1971, pp. 3–62 (Chapter 12);  
(b) R.A. Sheldon, J.K. Kochi, Mechanisms of metal-catalyzed oxidation of organic compounds in the liquid phase, *Oxid. Combust. Rev.* 5 (1973) 135–242;  
(c) R.A. Sheldon, J.K. Kochi, Metal catalyzed oxidations of organic compounds in the liquid phase: a mechanistic approach, *Adv. Catal.* 25 (1976) 272–341;  
(d) C.A. Tolman, J.D. Duliner, M.J. Nappa, N. Herron, in: C.L. Hill (Ed.), *Activation and Functionalization of Alkanes, Alkane Oxidation Studies in DuPont's Central Research Department*, Wiley, New York, 1989, pp. 303–360 (Chapter X).
- [25] Y. Lin, K. Nomiya, R.G. Finke, *Inorg. Chem.* 32 (1993) 6040.
- [26] (a) A. Fusi, R. Ugo, F. Fox, A. Pasini, S. Cenini, *J. Organomet. Chem.* 26 (1971) 417;  
(b) K. Takao, Y. Fujiwara, T. Imanaka, S. Teranishi, *Bull. Chem. Soc. Jpn.* 43 (1970) 1153.
- [27] A. Harrimasn, J.M. Thomas, G.R. Milward, *Nouv. J. Chem.* 11/12 (1987) 757.
- [28] D.J. Edlund, Ph.D. Thesis, University of Oregon, September 1987.
- [29] (a) M.N. Vargaftik, V.P. Zagorodnikov, I.P. Stolyarov, A.L. Chuvilin, V.I. Zaikovskiy, K.I. Zamaraev, G.I. Timofeeva, *J. Chem. Soc., Chem. Commun.* (1985) 937;  
(b) M.N. Vargaftik, I.P. Zagorodnikov, I.I. Stolarov, I. Moiseev, D.I. Kochubey, V.A. Likholobov, A.L. Chuvilin, K.I. Zamarev, *J. Mol. Catal.* 53 (1989) 315;  
(c) G. Schmid, B. Morun, J.-O. Malm, *Angew. Chem. Int. Engl. Ed.* 28 (1989) 778.
- [30] (a) H. Colfen, *Crit. Rev. Opt. Sci. Technol.* CR69 (1997) 525;  
(b) T.M. Laue, in: M.L. Johnson, G.K. Ackers (Eds.), *Methods in Enzymology*, Vol. 259, Academic Press, San Diego, 1995, p. 427;  
(c) S.E. Harding, *Meth. Mol. Biol.* 22 (1994) 75;  
(d) T.M. Laue, D.G. Rhodes, in: M.P. Deutscher (Ed.), *Methods in Enzymology*, Vol. 182, Academic Press, San Diego, 1990, p. 566.
- [31] A. Trovarelli, R.G. Finke, *Inorg. Chem.* 32 (1993) 6034.
- [32] H. Weiner, R.G. Finke, *J. Am. Chem. Soc.* 121 (1999) 9831.
- [33] (a) A.A. Frimer, *J. Org. Chem.* 19 (1977) 3194;  
(b) O.L. Magelli, C.S. Shepard, in: D. Swern (Ed.), *Organic Peroxides*, Vol. I, Wiley/Interscience, New York, 1970, pp. 1–19;  
(c) R. Hiatt, *Organic Peroxides*, Vol. II, Wiley/Interscience, New York, pp. 1–39, 114–115;  
(d) A.G. Davies, *Organic Peroxides*, Butterworths, London, 1961, pp. 1–41;  
(e) A.G. Tobelsky, R.B. Mesrobian, *Organic Peroxides*, Interscience, New York, 1954, pp. 1–11;  
(f) L.W. Fine, M. Grayson, V.H. Suggs, *J. Organomet. Chem.* 22 (1970) 219.
- [34] T.M. Laue, in: M.L. Johnson, G.K. Ackers (Eds.), *Methods in Enzymology*, Vol. 259, Academic Press, San Diego, 1995, p. 427.